



BNL-114192-2017-JA

Standard Model EFT and Extended Scalar Sectors

S. Dawson, C. W. Murphy

Submitted to Physical Review D

July 2017

Physics Department

Brookhaven National Laboratory

**U.S. Department of Energy
USDOE Office of Science (SC),
High Energy Physics (HEP) (SC-25)**

Notice: This manuscript has been co-authored by employees of Brookhaven Science Associates, LLC under Contract No. DE-SC0012704 with the U.S. Department of Energy. The publisher by accepting the manuscript for publication acknowledges that the United States Government retains a non-exclusive, paid-up, irrevocable, world-wide license to publish or reproduce the published form of this manuscript, or allow others to do so, for United States Government purposes.

DISCLAIMER

This report was prepared as an account of work sponsored by an agency of the United States Government. Neither the United States Government nor any agency thereof, nor any of their employees, nor any of their contractors, subcontractors, or their employees, makes any warranty, express or implied, or assumes any legal liability or responsibility for the accuracy, completeness, or any third party's use or the results of such use of any information, apparatus, product, or process disclosed, or represents that its use would not infringe privately owned rights. Reference herein to any specific commercial product, process, or service by trade name, trademark, manufacturer, or otherwise, does not necessarily constitute or imply its endorsement, recommendation, or favoring by the United States Government or any agency thereof or its contractors or subcontractors. The views and opinions of authors expressed herein do not necessarily state or reflect those of the United States Government or any agency thereof.

Standard Model EFT and Extended Scalar Sectors

Sally Dawson^{*} and Christopher W. Murphy[†]

Department of Physics, Brookhaven National Laboratory, Upton, N.Y., 11973, U.S.A.

One of the simplest extensions of the Standard Model is the inclusion of an additional scalar multiplet, and we consider scalars in the $SU(2)_L$ singlet, triplet, and quartet representations. We examine models with heavy neutral scalars, $m_H \sim 1 - 2$ TeV, and the matching of the UV complete theories to the low energy effective field theory. We demonstrate the agreement of the kinematic distributions obtained in the singlet models for the gluon fusion of a Higgs pair with the predictions of the effective field theory. The restrictions on the extended scalar sectors due to unitarity and precision electroweak measurements are summarized and lead to highly restricted regions of viable parameter space for the triplet and quartet models.

I. INTRODUCTION

The discovery of the Higgs boson at the LHC marks the beginning of the exploration of the nature of electroweak symmetry breaking. Our knowledge of the structure of the scalar potential remains primitive – there are no experimental measurements of the Higgs self-couplings and extended Higgs sectors can easily be made consistent with LHC data on single Higgs production and searches for heavy neutral scalars. The cleanest mechanism for obtaining information on the Higgs tri-linear coupling is a measurement of double Higgs production from gluon fusion. In the Standard Model (SM), the rate for double Higgs production is exceedingly small, presenting a challenge even for the high luminosity LHC.

The simplest extension of the SM scalar sector is the inclusion of an additional scalar multiplet, ϕ . If these new scalar multiplets, ϕ , have light neutral scalars in addition to the 125 GeV Higgs boson, the new scalars can be studied by direct production and they can also contribute resonant signatures to double Higgs production. Alternatively, if the new neutral scalars are heavy, $M_\phi \gg m_h$, their contributions to low scale physics can be captured in an effective field theory framework, with the largest effects coming from dimension-6 operators [1–8].

We concentrate on UV complete models with scalar sectors that have renormalizable couplings to the SM Higgs doublet. The list of such representations is rather short, and the parameters of these models are tightly restricted by the requirements of perturbative unitarity and agreement with precision electroweak measurements. We consider scalars that are $SU(3)_C$ singlets and $SU(2)_L$ singlets, triplets, and quartets. (The interesting case of additional $SU(2)_L$ doublets has been extensively studied in the literature [3–13].) Using standard techniques [1, 3], the heavy ϕ can be integrated out, leading to predictions for the effective field theory dimension-6 coefficients corresponding to a given extended scalar model. We restrict ourselves to contributions that arise at tree level. Furthermore, we assume no large non-linearities are generated when the heavy ϕ is integrated out. That is to say, we are using the SM Effective Field Theory (SMEFT), not Higgs Effective Field Theory (HEFT) [14–16].

An effective field theory has an expansion in powers of $(\text{Energy})^2/\Lambda^2$, where Λ is a high scale UV cut-off. At large values of the energy, kinematic distributions in the SMEFT can be expected to diverge from the exact low energy results [17, 18]. A well known example in the case of $gg \rightarrow hh$ is the failure of the $m_t \rightarrow \infty$ limit to reproduce the exact cross section and invariant mass distribution [19–21]. The SMEFT operators have different energy dependences in the high energy limit, and kinematic distributions could potentially distinguish between the contributions of different dimension-6 operators [22–24]. We study the accuracy of the effective field theory for reproducing the predictions of UV complete models with heavy scalar singlets for the $gg \rightarrow hh$ process and compare the p_T spectrum and the M_{hh} distributions in the SMEFT and the UV complete singlet models [21, 25–29]. Analogous studies have shown good agreement for single Higgs production in selected models with extended scalar sectors [5, 6].

The scalar triplet model violates custodial $SU(2)$ and all of the SMEFT coefficients are proportional to

^{*}Electronic address: dawson@bnl.gov

[†]Electronic address: cmurphy@quark.phy.bnl.gov

this violation and hence are forced to be small [10, 30–33]. The combined requirements from measurements of the ρ parameter and perturbative unitarity lead to models that are indistinguishable from the SM through either single or double Higgs production. The quartet models [34] also violate custodial $SU(2)$ and we demonstrate that these models have extremely restricted regions of viable parameter space when perturbative unitarity is enforced.

In Section II, we review the framework of the SMEFT with details given in Appendix A, while Section III has descriptions of the extended scalar sectors we consider. Further details of the models are contained in Appendix B. Section IV contains discussions of limits on the parameters of the scalar sectors from the ρ parameter, single Higgs production, and the requirement of perturbative unitarity. In particular, a discussion of limits on the SMEFT coefficients in models with extended Higgs sectors from single Higgs production is given in Section IV B. The numerical comparison of the SMEFT and extended scalar models for double Higgs production is in Section V, with conclusions in Section VI.

II. STANDARD MODEL EFFECTIVE FIELD THEORY

The Lagrangian we consider can be written as

$$\mathcal{L}_{SMEFT} = \mathcal{L}_{SM} + \mathcal{L}^{(5)} + \mathcal{L}^{(6)} + \dots \quad (1)$$

where $\mathcal{L}^{(n)}$ has dimension- n and can be parameterized as $\mathcal{L}^{(n)} = \sum_i \frac{c_i^{(n)}}{v^{n-4}} O_i^{(n)}$.

Including only the third generation fermions and neglecting possible mixing with the lighter generations, the Higgs sector of the SM is given by

$$\begin{aligned} \mathcal{L}_{SM} \supset \mathcal{L}_H &= (D_\mu H)^\dagger (D^\mu H) - V_{SM}(H) \\ &\quad - \left[y_b (\bar{q}_L b_R H) + y_t (\bar{q}_L t_R \tilde{H}) + y_\tau (\bar{l}_L \tau_R H) + \text{h.c.} \right], \\ V_{SM}(H) &= -\mu^2 (H^\dagger H) + \lambda (H^\dagger H)^2, \end{aligned} \quad (2)$$

where \bar{q}_L and \bar{l}_L are the left-handed $(t, b)_L$ and $(\nu, \tau)_L$ doublets, $\tilde{H} \equiv i\sigma_2 H^*$, and the $SU(2)_L$ doublet H is parameterized as,

$$H \equiv \begin{pmatrix} H_1 \\ H_2 \end{pmatrix} \equiv \begin{pmatrix} w^+ \\ \frac{v_h + h' + iz}{\sqrt{2}} \end{pmatrix}. \quad (3)$$

We are interested in the dimension-6 CP-conserving operators generated at tree level by extended scalar sectors, which takes the form,

$$\begin{aligned} \mathcal{L}^{(6)} &= \sum_i \frac{c_i}{v^2} O_i \supset \mathcal{L}_H^{(6)} \\ \mathcal{L}_H^{(6)} &= \frac{c_H}{2v^2} \partial_\mu (H^\dagger H) \partial^\mu (H^\dagger H) + \frac{c_T}{2v^2} \left| H^\dagger \overleftrightarrow{D}_\mu H \right|^2 - \frac{c_6 \lambda}{v^2} (H^\dagger H)^3 \\ &\quad + \frac{(H^\dagger H)}{v^2} \left[c_b y_b (\bar{q}_L b_R H) + c_t y_t (\bar{q}_L t_R \tilde{H}) + c_\tau y_\tau (\bar{l}_L \tau_R H) + \text{h.c.} \right], \end{aligned} \quad (4)$$

where $H^\dagger \overleftrightarrow{D}_\mu H \equiv H^\dagger D_\mu H - (D_\mu H^\dagger) H$. In the models we consider $c_t = c_b = c_\tau \equiv c_f$ at tree-level and none of the extended scalar models we consider generate $H^\dagger H V_{\mu\nu}^A V^{A\mu\nu}$ (V is the $SU(3)_C$, $SU(2)_L$ or $U(1)$ gauge boson) at tree level, so they are not included in Eq. (4). Minimizing the potential in Eq. (2) yields the constraint

$$\mu^2 = \lambda v^2 \left(1 + \frac{3}{4} c_6 \right), \quad (5)$$

where $v \approx 246$ GeV is the vacuum expectation value (vev) of the Higgs field. With this normalization the coefficients of the operators appearing in Eq. (4) are of order v^2/Λ^2 , where again Λ is the cutoff of the effective theory. In addition to the previously mentioned energy expansion, there is also a mass gap, $v^2 < \Lambda^2$.

We use the basis of Ref. [35], as it has a convenient normalization for our purposes. It is straightforward to convert this basis into a different one, *e.g.* [36], and Appendix A contains information about operator bases and other SMEFT details. We are primarily interested in the leading order (LO) EFT effects, which generally means dimension-6 operators generated at tree level. We note that at one-loop the renormalization group (RG) evolution of the operators O_H and O_T generates operators of the form $\psi^2 H^2 D$ [37–39]. The subset of dimension-6 operators considered in Eq. (4) is otherwise closed under RG evolution at one-loop.

The kinetic energy for the Higgs boson, h' , in Eq. (1) is not canonically normalized. A field redefinition can be made to correctly normalize the kinetic energy¹ and eliminate derivative interactions [40, 41]

$$h' = h \left[1 - \frac{c_H}{2} \left(1 + \frac{h}{v} + \frac{h^2}{3v^2} \right) \right], \quad (6)$$

$$\partial_\mu h' = \partial_\mu h \left[1 - \frac{c_H}{2} \left(1 + \frac{h}{v} \right)^2 \right].$$

Using Eq. (6) the Higgs boson Lagrangian takes the form

$$\begin{aligned} \mathcal{L}_h = & \frac{1}{2} (\partial_\mu h)^2 - \frac{1}{2} m_h^2 h^2 - \frac{m_h^2}{2v} \left(1 + c_6 - \frac{3}{2} c_H \right) h^3 \\ & - \frac{m_h^2}{8v^2} \left(1 + 6c_6 - \frac{25}{3} c_H \right) h^4 - \frac{m_h^2}{48v^4} (3c_6 - 4c_H) h^5 (h + 6v), \end{aligned} \quad (7)$$

with $m_h \approx 125$ GeV. There are also modifications to the Yukawa sector from Eq. (6)

$$\mathcal{L}_{y_t} = -m_t \bar{t} t \left[1 + \left(1 - \frac{c_H + 2c_t}{2} \right) \frac{h}{v} - \frac{c_H + 3c_t}{2} \left(\frac{h^2}{v^2} + \frac{h^3}{3v^3} \right) \right], \quad (8)$$

and similarly for the other SM fermions.

III. EXTENDED SCALAR SECTORS

We consider a number of extensions of the SM where a single new spin-zero multiplet, ϕ , is added to the SM and require that there is a renormalizable interaction with the SM H doublet that is linear in ϕ . There is a sizable literature on integrating out heavy scalars and studying their SMEFT contributions, see for instance [3–7, 10–13]. The models we consider are: a real singlet ($\mathbf{1}_0$), a real triplet ($\mathbf{3}_0$), a complex triplet ($\mathbf{3}_1$), and two quartets: quartet₁ ($\mathbf{4}_{1/2}$) and quartet₃ ($\mathbf{4}_{3/2}$). The numbers in parentheses are the $SU(2)_L \times U(1)_Y$ quantum numbers of the new scalars, all of which are color singlets. These models only generate dimension-6 operators of the form H^6 and $H^4 D^2$ at tree level (where D is the $SU(2)_L \times U(1)_Y$ covariant derivative). As such they are good candidates to be discovered through deviations in double Higgs production from the SM predictions.

The potential can schematically be written as (see also [34])

$$V(H, \phi) = V_{SM}(H) + V_{Z_2}(H, \phi) + V_{\mathbb{Z}_3}(H, \phi), \quad (9)$$

where ϕ is the new scalar, and V_{SM} is given in Eq. (2). For a real valued ϕ , the Z_2 preserving potential has the following form

$$V_{Z_2}(H, \phi) = \frac{1}{2} M^2 \phi^a \phi^a + \lambda_\alpha H^\dagger H \phi^a \phi^a + \lambda_\beta (\phi^a \phi^a)^2, \quad (10)$$

where a are the $SU(2)_L$ indices, and for a complex valued ϕ there may be multiple α and/or β -type interactions. Additionally, when ϕ is complex, there is no factor of one-half in front of the mass term,

¹ We work to linear order in the coefficients, c_i .

Model	\mathbf{c}_H	$\mathbf{c}_6 \lambda_{SM}$	\mathbf{c}_T	\mathbf{c}_F
Real Singlet w/ explicit \mathbb{Z}_2	$\frac{m_1^2 v^2}{M^4}$	$\frac{m_1^2 v^2}{M^4} (\lambda_\alpha - \frac{m_1 m_2}{M^2})$	0	0
Real Singlet w/ spontaneous \mathbb{Z}_2	$\left(\frac{\lambda_\alpha v}{4\lambda_\beta v_\phi}\right)^2$	0	0	0
2HDM	0	\checkmark	0	\checkmark
Real Triplet	$-\frac{m_1^2 v^2}{2M^4}$	$\frac{m_1^2 v^2 \lambda_\alpha}{4M^4}$	$\frac{m_1^2 v^2}{4M^4}$	$\frac{m_1^2 v^2}{4M^4}$
Complex Triplet	$-\frac{m_1^2 v^2}{2M^4}$	$\frac{m_1^2 v^2}{2M^4} (\lambda_{\alpha 1} - \frac{\lambda_{\alpha 2}}{2})$	$-\frac{m_1^2 v^2}{2M^4}$	$\frac{m_1^2 v^2}{2M^4}$
Quartet ₁	0	$-\frac{\lambda_1^2 v^2}{M^2}$	0	0
Quartet ₃	0	$-\frac{\lambda_1^2 v^2}{M^2}$	0	0

TABLE I: The dimension-6 operators from Eq. (4) that are generated at tree level in the models under consideration. Here $\lambda_{SM} = m_h^2/2v^2$. The 2HDM is listed for the sake of comparison (it additionally generates four-fermion operators). Note that the factors of v are due to the normalization of Eq. (4).

and $\phi^a \phi^a$ should be replaced with $\phi^{a\dagger} \phi^a$. Depending on the $SU(2)_L$ representation of ϕ , the Z_2 violating potential contains one of the following interactions

$$V_{\mathbb{Z}_2} \sim m_1 H^2 \phi \quad \text{or} \quad V_{\mathbb{Z}_2} \sim \lambda_1 H^3 \phi. \quad (11)$$

If ϕ is a singlet there can also be a tadpole term and a cubic self-interaction, both of which violate the Z_2 symmetry.

The essential features of each model are listed below. Additional details have been relegated to Appendix B. We define the angle α to characterize the mixing between the neutral, CP -even components of H and ϕ

$$\begin{pmatrix} h \\ \mathcal{H} \end{pmatrix} = \begin{pmatrix} \cos \alpha & -\sin \alpha \\ \sin \alpha & \cos \alpha \end{pmatrix} \begin{pmatrix} h' \\ \varphi \end{pmatrix}, \quad (12)$$

where $\text{Re}(H_2) = \frac{v_h + h'}{\sqrt{2}}$ and $\text{Re}(\phi^0) = v_\phi + \varphi$, and v_h and v_ϕ are the vevs of H and ϕ , respectively. In all of the models we consider, a non-zero value of α leads to a universal modification of the Higgs couplings to SM particles (excluding the Higgs self-couplings). This angle has been bounded from the single Higgs signal strengths by the ATLAS collaboration, with the result $\cos \alpha > 0.94$ at the 95% confidence level (CL) [42].

With the above definitions of the vevs of H and ϕ , the electroweak (EW) vev is given by

$$v^2 = v_h^2 + 2 [t(\phi)(t(\phi) + 1) - t_3(\phi)^2] v_\phi^2, \quad (13)$$

where $t(i)$, $t_3(i)$, and v_i are the representation under $SU(2)_L$ of the i th multiplet, the neutral component of the i th multiplet, and the vev of the i th multiplet, respectively. When ϕ is a singlet $v_h = v$, and we define

$$\tan \beta_s = v_h / v_\phi. \quad (14)$$

For higher $SU(2)_L$ representations, we define the mixing angle between the two vevs as

$$v_h = v \cos \beta, \quad v_\phi = v \sin \beta / \sqrt{2 [t(\phi)(t(\phi) + 1) - t_3(\phi)^2]}. \quad (15)$$

The potentials listed below are understood to be in addition to the SM-like potential, V_{SM} . Given these interactions, standard methods exist to determine which operators in the SMEFT are generated at tree level in a given model [3, 10]. The dimension-6 results are compiled in Table I.

From Tab. I we see that taking λ_1 or $m_1 \rightarrow 0$ while holding the other parameters fixed, or sending $M \rightarrow \infty$ also while keeping the other parameters fixed, causes the new scalar multiplet to decouple.²

² The analogs of m_1 and M in the singlet model with spontaneous Z_2 breaking are λ_α and v_ϕ , respectively.

Model	c_H	$c_6 \lambda_{SM}$	c_T	c_f
Real Singlet w/ explicit Z_2	$\tan^2 \alpha$	$\tan^2 \alpha \left(\lambda_\alpha - \frac{m_2}{v} \tan \alpha \right)$	0	0
Real Singlet w/ spontaneous Z_2	$\tan^2 \alpha$	0	0	0
Real Triplet	$-\frac{8 \sin^2 \beta m_{H+}^4}{m_H^4}$	$\frac{4 \sin^2 \beta m_{H+}^6}{m_H^4 v^2}$	$\frac{4 \sin^2 \beta m_{H+}^4}{m_H^4}$	$\frac{4 \sin^2 \beta m_{H+}^4}{m_H^4}$
Complex Triplet	$-\frac{4 \sin^2 \beta m_A^4}{m_H^4}$	$\frac{8 \sin^2 \beta m_A^6}{m_H^4 v^2}$	$-\frac{4 \sin^2 \beta m_A^4}{m_H^4}$	$\frac{4 \sin^2 \beta m_A^4}{m_H^4}$
Quartet ₁	0	$\frac{24 \tan^2 \beta m_A^4}{7 m_H^2 v^2}$	0	0
Quartet ₃	0	$\frac{8 \tan^2 \beta m_A^4}{3 m_H^2 v^2}$	0	0

TABLE II: Approximate tree-level expressions for the dimension-6 Wilson coefficients in terms of physical masses and mixing angles. We assume a common mass for the heavy Higgses – except for m_A (m_{H+} for the real triplet), which is associated with the alignment without decoupling limit – and take this mass to be heavy. Additionally for the triplets and quartets, we assume α is sufficiently small such that it can be neglected. Non-zero values for c_T arise in the quartet models at dimension-8, and they have the same parametric form as the (dimension-6) contribution to c_T in the complex triplet model.

These are the analogs of the alignment without decoupling limit, and the decoupling limit of the 2HDM, respectively [8, 9].

We also give approximate expressions for the dimension-6 Wilson coefficients in terms of physical masses and mixing angles in Table II. We assume a common mass for the heavy Higgses – except for m_A (m_{H+} for the real triplet), which is associated with the alignment without decoupling limit – and take this mass to be heavy. The heavy mass limit needs to be taken with $m_A^2 \sin^2 \beta$ fixed for a weakly interacting theory. Additionally for the triplets and quartets, we assume α is sufficiently small such that it can be neglected.

- **Singlets:** The most general renormalizable potential is

$$V_s = \frac{1}{2} M^2 \phi^2 + m_1 H^\dagger H \phi + m_2 \phi^3 + m_3^3 \phi + \lambda_\alpha H^\dagger H \phi^2 + \lambda_\beta \phi^4. \quad (16)$$

If $m_{1,2,3} \rightarrow 0$, the potential exhibits an explicit Z_2 symmetry. In the absence of a Z_2 symmetry, the parameters can be redefined to eliminate a vev for ϕ . In terms of the masses of the Higgs bosons and the mixing angle α , the Wilson coefficient c_H is the same whether or not there is an explicit Z_2 symmetry,

$$c_H = \frac{(m_H^2 - m_h^2)^2 \sin^2 2\alpha}{(m_H^2 + m_h^2 + (m_H^2 - m_h^2) \cos 2\alpha)^2}. \quad (17)$$

The limiting forms of Eq. (17) are

$$c_H = \begin{cases} \tan^2 \alpha & m_H \rightarrow \infty \\ \left(1 - \frac{m_h^2}{m_H^2}\right)^2 \alpha^2 & \alpha \rightarrow 0 \end{cases} \quad (18)$$

When the EFT coefficients are expressed in terms of the mass eigenstate parameters, we see from Eq. (18) that sending $\alpha \rightarrow 0$ is equivalent to taking the alignment without decoupling limit, but sending $m_H \rightarrow \infty$ is not the same as taking the decoupling limit.

- **Real Singlet with Explicit Z_2 Breaking:** When the Z_2 symmetry for ϕ is explicitly broken, the parameters in Eq. (16) can be redefined such that ϕ does not get a vev. Parameter space exists such that this the deepest of the possible vacua in the theory [21, 43]. In addition, we redefine M to allow for an easier comparison with the spontaneous symmetry breaking case. The potential is then,

$$V_s = \frac{1}{2} M^2 \phi^2 + m_1 \left(H^\dagger H - \frac{v^2}{2} \right) \phi + m_2 \phi^3 + \lambda_\alpha \left(H^\dagger H - \frac{v^2}{2} \right) \phi^2 + \lambda_\beta \phi^4. \quad (19)$$

In this case,

$$\lambda_{SM} c_6 = c_H \left(\lambda_\alpha - \frac{m_1 m_2}{M^2} \right), \quad (20)$$

and λ_α and m_2 are free parameters limited by perturbative unitarity, precision electroweak measurements, and the minimization of the potential, while m_1 can be expressed in terms of m_h , m_H and α . For large M , $M \sim m_H$.

- **Real Singlet with Spontaneous Z_2 Breaking:** In the case of an explicit Z_2 symmetry, ϕ develops a vev, $\phi = v_\phi + \varphi$. This spontaneously breaks the symmetry, and leads to the following potential:

$$V_s = \lambda_\alpha \left(H^\dagger H - \frac{v^2}{2} \right) (\phi^2 - v_\phi^2) + \lambda_\beta (\phi^2 - v_\phi^2)^2. \quad (21)$$

In this scenario c_6 vanishes at tree level due to the explicit Z_2 symmetry, but c_H is still non-zero [5].

- **Triples:** We use an adjoint notation for the triplets

$$\phi = \phi^a T^a = \frac{1}{2} \begin{pmatrix} \phi^Y & \sqrt{2}\phi^{Y+1} \\ \sqrt{2}\phi^{Y-1} & -\phi^Y \end{pmatrix}, \quad (22)$$

where Y is the hypercharge of the triplet, and $T^a = \sigma^a/2$ with σ^a being the Pauli matrices. All of the Wilson coefficients in the triplet models are proportional to c_T , indicating there is limited potential for these models to modify double-Higgs production since c_T is constrained by the ρ parameter, see Eq. (36).

- **Real Triplet:** The real $SU(2)_L$ triplet is hypercharge neutral. The potential in this case is

$$V_{tr} = \frac{1}{2} M^2 \phi^a \phi^a + m_1 H^\dagger T^a H \phi^a + \lambda_\alpha H^\dagger H \phi^a \phi^a + \lambda_\beta (\phi^a \phi^a)^2. \quad (23)$$

The Wilson coefficients are all proportional to $\rho - 1$, see Eq. (37) in what follows:

$$c_T = c_f = -\frac{c_H}{2} = \rho - 1, \quad c_6 \lambda_{SM} = (\rho - 1) \lambda_\alpha. \quad (24)$$

- **Complex Triplet:** The complex triplet has hypercharge one. Much of the discussion is similar to the real case. The potential is

$$\begin{aligned} V_{tc} = & M^2 \phi^{\dagger a} \phi^a + m_1 \left(H^\dagger T^a \tilde{H} \phi^a + \text{h.c.} \right) + \lambda_{\alpha 1} H^\dagger H \phi^{\dagger a} \phi^a \\ & + i \lambda_{\alpha 2} H^\dagger T^a H \epsilon^{abc} \phi^{\dagger b} \phi^c + \lambda_{\beta 1} (\phi^{\dagger a} \phi^a)^2 - \lambda_{\beta 2} \epsilon^{abc} \epsilon^{ade} \phi^{\dagger b} \phi^c \phi^{\dagger d} \phi^e. \end{aligned} \quad (25)$$

The relations between the coefficients in the complex triplet case are different than in the real case, but again all of the Wilson coefficients are proportional to $\rho - 1$:

$$c_T = -c_f = c_H = \rho - 1, \quad c_6 \lambda_{SM} = (1 - \rho) \left(\lambda_{\alpha 1} - \frac{\lambda_{\alpha 2}}{2} \right). \quad (26)$$

- **Quartets:** The $SU(2)_L$ quartets of interest have either hypercharge $Y = 3/2$ or $1/2$. In both cases, the Z_2 preserving part of the potential is

$$\begin{aligned} V_{q,Z_2} = & M^2 \phi^{*ijk} \phi_{ijk} + \lambda_{\alpha 1} H^{*i} H_i \phi^{*ljk} \phi_{ljk} + \lambda_{\alpha 2} H^{*i} H_k \phi^{*ljk} \phi_{lji} \\ & + \lambda_{\beta 1} (\phi^{*ijk} \phi_{ijk})^2 + \lambda_{\beta 2} \phi^{*ijk} \phi_{ijn} \phi^{*lmn} \phi_{lmk}. \end{aligned} \quad (27)$$

We use a symmetric tensor notation, $\phi = \phi_{(ijk)}$ [44], where the indices are summed over. Since the Young's Tableau for $SU(2)$ only has one row, and representations are symmetric with respect to exchange of blocks of a given row, a $2j + 1$ $SU(2)$ multiplet can be written as a $2j$ index symmetric tensor.

- **Quartet₁:** In the $Y = 1/2$ case, the Z_2 breaking term is

$$V_{q_1, Z_2} = -\lambda_1 (\phi^{*ijk} H_i H_j \epsilon_{kl} H^{*l} + \text{h.c.}). \quad (28)$$

The only dimension-6 operator generated is [3]

$$c_6 \lambda_{SM} = -\frac{\lambda_1^2 v^2}{M^2}. \quad (29)$$

The quartet is the only model considered here that contains cubic interactions of the SM H doublet with ϕ , leading to dimension-6 coefficients of $\mathcal{O}(\frac{1}{M^2})$. The same value for c_6 is generated in the $Y = 3/2$ case.

Once EW symmetry is broken c_T is generated at tree level through a dimension-8 operator. When H gets a vev, ϕ is forced to get a vev. Using the results of Appendix B we find

$$v_\phi \approx \frac{\sqrt{3} \lambda_1 v_h^3}{6M^2}. \quad (30)$$

The vev of ϕ leads to the dimension-8 contribution to c_T ,

$$c_T = -\frac{1}{2} \frac{v^2}{M^2} (c_6 \lambda_{SM}). \quad (31)$$

We see that the tree level value for c_T is 0 at dimension-6, and receives a non-zero tree level contribution only at dimension-8.

– **Quartet₃**: In the $Y = 3/2$ case, the Z_2 breaking part of the potential is

$$V_{q_3 \mathbb{Z}_2} = -\lambda_1 (\phi^{*ijk} H_i H_j H_k + \text{h.c.}). \quad (32)$$

In this case the vev of ϕ is

$$v_\phi \approx \frac{\lambda_1 v_h^3}{2M^2}, \quad (33)$$

leading to a tree level dimension-8 contribution,

$$c_T = \frac{3}{2} \frac{v^2}{M^2} (c_6 \lambda_{SM}). \quad (34)$$

Inclusion of these dimension-8 contributions to c_T in a global fit would require a complete treatment of all the dimension-8 operators, along with loop contributions from the dimension-6 operators, which is beyond the scope of this work. They are included here to make the general point that there is no symmetry requiring ρ to be 0 in the quartet models once electroweak symmetry is broken.

The set of models considered in this work only generate dimension-6 operators of the form H^6 , $H^4 D^2$ at tree level. This is not obvious from Tab. I because we are using a non-redundant set of operators. An additional scalar operator, O_R , is generated by some of the models. However, when O_R is eliminated from our operator basis, see Appendix A, operators of the form $\psi^2 H^3$ are generated in addition to purely scalar operators. In contrast with the models we consider, the Two-Higgs Doublet Model (2HDM) generically leads to operators of the form $\psi^2 H^3$, ψ^4 , even if redundant operators are retained.³ Due to this complication, and the fact that the 2HDM is extremely well studied, we do not analyze it in this work. See Refs. [3–6, 13, 45] for some studies of the 2HDM in an effective field theory context.

For the singlet model, we separately considered the cases of explicit and spontaneous Z_2 symmetry breaking. What happens when a Z_2 symmetry is imposed on a triplet or higher representation? If ϕ gets a vev, there is a leftover global $U(1)$ symmetry that leaves the CP -odd Higgs boson massless.⁴ There are two ways out of this problem. The first solution is to not allow the additional multiplet to get a vev. This is the analog of the inert 2HDM [46]. In this case, no dimension-6 operators are generated at tree level, both in the inert 2HDM and in the higher representation models as well. Alternatively, the pseudoscalar will acquire a mass in the higher representation models if the Z_2 symmetry is softly broken. In the triplet models it is possible to achieve a soft breaking of the Z_2 symmetry, just as in the 2HDM, through the interaction with coefficient m_1 . This is not the case for the quartet models where the only (renormalizable) Z_2 violating interaction is marginal.

³ The complex triplet can also interact with SM fermions. In particular, there could be the lepton number violating interaction, $\bar{\ell}_L \phi^\dagger (i\sigma^2 \ell_L^c) + \text{h.c.}$ We assume the Yukawa coupling associated with this interaction is negligibly small, consistent with the existence of tiny neutrino masses.

⁴ In the real triplet model, it is the charged Higgs boson that is massless in this scenario.

IV. CONSTRAINTS

A. The Rho Parameter

The ρ parameter is defined as the ratio of neutral to charged currents at low energies [47]

$$\rho = \frac{M_W^2}{M_Z^2 \cos^2 \theta_W}. \quad (35)$$

A recent global fit to EW precision data yielded the value [48]

$$\rho_{\text{exp.}} = 1 + (3.6 \pm 1.9) \cdot 10^{-4}. \quad (36)$$

In terms of dimension-6 operators, the ρ parameter takes the form

$$\rho = 1 + c_T. \quad (37)$$

Alternatively, the tree level contribution in the extended scalar models can be written in terms of the Higgs vevs [49]

$$\rho = \frac{\sum_i [t(i)(t(i)+1) - t_3(i)^2] v_i^2}{2 \sum_i t_3(i)^2 v_i^2}. \quad (38)$$

The numerator of Eq. (38) is equivalent to $v^2/2$ (with $v \approx 246$ GeV). We can use this fact to eliminate one term from the sum in Eq. (38), say the $i = 1$ term. If the $i = 1$ $SU(2)_L$ multiplet is taken to be a doublet, possibly SM-like, Eq. (38) simplifies to

$$\rho = \frac{v^2}{v^2 - 2 \sum_{i>1} [t(i)(t(i)+1) - 3t_3(i)^2] v_i^2}. \quad (39)$$

We can compare the calculations of ρ in the unbroken and broken phases of the theories, Eqs. (37) and (39), respectively. Using the results of Appendix B we have checked that for the triplet models, with the reasonable approximations $v_\phi \ll v$ and $v_h \approx v$, the calculations of ρ agree in the two different phases. On the other hand, in the quartet models the predictions for ρ in the broken phase and the dimension-6 contribution to the unbroken phase do not agree. A non-zero value of $\rho - 1$ is generated, as in Eq. 39, in the broken phase by the non-zero value of v_ϕ , while $\rho = 1$ at dimension-6 in the EFT. This mis-match is understood by noting that at the tree level in the EFT, a non-zero value of $\rho - 1$ is generated by dimension-8 operators.

In terms of the mixing angle β , the tree level contribution of each model to the ρ parameter is given in Table III. Also shown in Tab. III is the bound on β from Eq. (36). We have included the dimension-8 contribution for the quartet model, since this is the leading tree level contribution to the experimentally well-measured ρ parameter in the UV complete scalar theory. Since the global fit prefers a value for ρ slightly greater than one, the models that contribute positively to ρ are somewhat less constrained than those that contribute negatively to ρ .

As previously mentioned, all of the dimension-6 operators generated at tree level in the triplet models are proportional to c_T , which constrains the size of those Wilson coefficients to be small.

One way to understand why the triplet and quartet models yield a value for the ρ parameter different from unity is to make a comparison with the SM. In particular, the Higgs sector of the SM possesses an accidental $SU(2)_L \times SU(2)_R$ symmetry. When EW symmetry is broken, the accidental symmetry is broken down to its vectorial subgroup, which is the custodial symmetry. This symmetry enforces $\rho = 1$ at tree level in the SM. Adding a single triplet or quartet field to the SM is problematic from this point of view because those fields do not have definite representations under the $SU(2)_R$ component of the accidental symmetry of the SM, and thus $\rho = 1$ cannot be enforced at tree level. A resolution to this problem is to add two $SU(2)_L$ triplet fields to the SM that form a bi-triplet under $SU(2)_L \times SU(2)_R$, preserving custodial symmetry and the tree level $\rho = 1$ prediction. This is known as the Georgi-Machacek model [50, 51]. This procedure can be generalized to include higher $SU(2)_L$ representations, including quartets [52].

Model	ρ	3σ upper limit on β
Singlet	1	none
2HDM	1	none
Real Triplet	$\sec^2 \beta$	0.030
Complex Triplet	$2(3 - \cos 2\beta)^{-1}$	0.014
Quartet ₁	$7(4 + 3 \cos 2\beta)^{-1}$	0.033
Quartet ₃	$(2 - \cos 2\beta)^{-1}$	0.010

TABLE III: The tree level contribution to ρ in a given model, and the corresponding 3σ upper limit on the mixing angle β . The contribution to the quartet models arises at dimension-8 and is included because it is the first non-zero tree level contribution to the well measured ρ parameter in the UV complete theory.

Signal strength	Value	Correlation matrix		μ_{SMEFT}
$\mu_{\text{ggF}+\text{tth}}^{\gamma\gamma}$	1.16 ± 0.26	1	-0.30	$1 - c_H + 0.01c_f$
$\mu_{\text{VBF}+\text{Vh}}^{\gamma\gamma}$	1.05 ± 0.43	-0.30	1	$1 - c_H + 2.01c_f$
$\mu_{\text{ggF}+\text{tth}}^{bb}$	1.15 ± 0.97	1	$4.5 \cdot 10^{-3}$	$1 - c_H + 2.55c_f$
$\mu_{\text{VBF}+\text{Vh}}^{bb}$	0.65 ± 0.30	$4.5 \cdot 10^{-3}$	1	$1 - c_H + 0.55c_f$
$\mu_{\text{ggF}+\text{tth}}^{\tau\tau}$	1.06 ± 0.58	1	-0.43	$1 - c_H + 2.55c_f$
$\mu_{\text{VBF}+\text{Vh}}^{\tau\tau}$	1.12 ± 0.36	-0.43	1	$1 - c_H + 0.55c_f$
$\mu_{\text{ggF}+\text{tth}}^{WW}$	0.98 ± 0.21	1	-0.14	$1 - c_H + 0.55c_f$
$\mu_{\text{VBF}+\text{Vh}}^{WW}$	1.38 ± 0.39	-0.14	1	$1 - c_H + 1.45c_f$
$\mu_{\text{ggF}+\text{tth}}^{ZZ}$	1.42 ± 0.35	1	-0.49	$1 - c_H + 0.55c_f$
$\mu_{\text{VBF}+\text{Vh}}^{ZZ}$	0.47 ± 1.37	-0.49	1	$1 - c_H + 1.45c_f$

TABLE IV: Higgs boson signal strengths from [54]. The right column has the signal strengths in the SMEFT for the operators in Eq. (4). The left three columns are adapted from [55].

B. Single Higgs Production

Quite generically, theories that modify the rate for double Higgs boson production will also modify the production rate for a single 125 GeV Higgs boson, as well as the Higgs boson's branching ratios. For the models with extended scalar sectors that we are interested in, measurements of the 125 GeV Higgs boson yield the bound $\cos \alpha > 0.94$ at the 95% CL [42]. This suppresses the production of the heavy neutral Higgs boson by $\sin^2 \alpha$ with respect to the SM rate, which is below the current experimental sensitivities [53]. We are interested in bounding the Wilson coefficients that affect single Higgs production, c_H and c_f that are generated in the extended scalar models. The fit is particularly simple in these models, since other potential dimension-6 operators affecting Higgs couplings are not generated.

For a given Higgs boson production and decay process, $i \rightarrow h \rightarrow f$, the signal strength is defined as

$$\mu_i^f = \mu_i \cdot \mu^f = \frac{\sigma(i \rightarrow h)}{(\sigma(i \rightarrow h))_{\text{SM}}} \cdot \frac{\text{Br}(h \rightarrow f)}{(\text{Br}(h \rightarrow f))_{\text{SM}}}. \quad (40)$$

We use the combined results of ATLAS and CMS based on 7 and 8 TeV data [54], which can be found in Table IV. The three leftmost columns of Tab. IV are adapted from Ref. [55], which obtains the values of the signal strengths from Table 13 of [54], and estimates the correlations between the signal strengths from Figure 14 of [54]. The rightmost column is the signal strength in the SMEFT for the operators in Eq. (4). For loop level processes, we use the approximate expressions for the signal strengths given in Ref. [56]. SM Higgs boson branching ratios and the total width are taken from Ref. [57].

The method of least squares is used to find the favored parameter space. The χ^2 function schematically is

$$\chi^2 \sim \left(\vec{\mu}_i^f - \vec{\mu}_{\text{SMEFT}} \right)^\top V^{-1} \left(\vec{\mu}_i^f - \vec{\mu}_{\text{SMEFT}} \right), \quad (41)$$

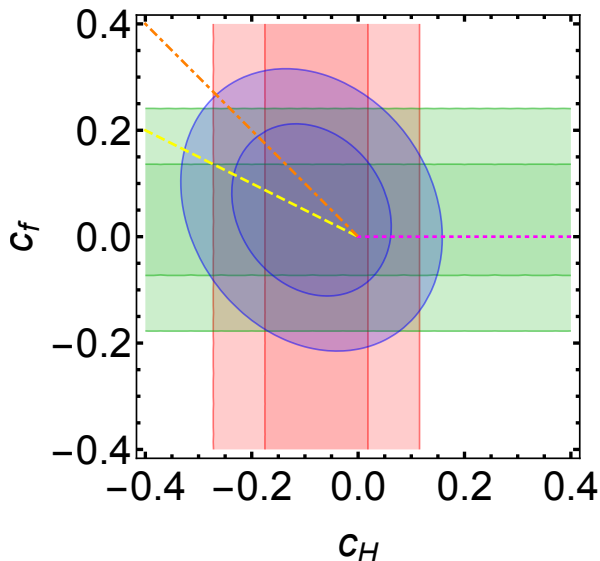


FIG. 1: Results of a χ^2 fit to Higgs data to limit c_H and c_f . The darker and lighter regions represent the 1σ and 2σ confidence regions, respectively. The magenta (dotted), yellow (dashed), and orange (dot-dashed) line segments correspond to the real singlet, real triplet, and complex triplet models, respectively. The signs of c_H and c_f are fixed in these models, which is why the line segments do not cover the whole plane.

where V is the covariance matrix of the experimental values. The parameter values that minimize χ^2 are

$$10^2 c_H = -8.8 \pm 9.9, \quad 10^2 c_f = 5.0 \pm 10.7 \quad (42)$$

$$r = \begin{pmatrix} 1 & -0.196 \\ -0.196 & 1 \end{pmatrix},$$

where the correlation matrix is denoted r to avoid confusion with the ρ parameter. Parameterizing the SMEFT coefficients as $c_H \sim \hat{c}_H \frac{v^2}{M^2}$, $c_f \sim \hat{c}_f \frac{v^2}{M^2}$, the 95% confidence level limits from Eq. (42) are,

$$-18 \left(\frac{M}{2 \text{ TeV}} \right)^2 < \hat{c}_H < 7 \left(\frac{M}{2 \text{ TeV}} \right)^2$$

$$-2 \left(\frac{M}{2 \text{ TeV}} \right)^2 < \hat{c}_f < 5 \left(\frac{M}{2 \text{ TeV}} \right)^2. \quad (43)$$

The SMEFT coefficients predicted in the previous sections from the extended scalar sectors are comfortably within the limits of Eq. (43).

The confidence regions for the estimated parameters are determined using $\chi^2 \leq \chi_{\min}^2 + \Delta\chi^2$, where the 1σ and 2σ regions are given by $\Delta\chi^2 = 1, 4$ (2.30, 6.18) when the number of parameters to be estimated is 1 (2). The results of this fit are shown in Fig. 1. The darker and lighter regions represent the 1σ and 2σ confidence regions, respectively. The red and green regions are fits to c_H or c_f with the other parameter fixed to zero, while the blue region is a simultaneous fit to both parameters. Also shown in Fig. 1 are the predictions for the real singlet (magenta, dotted), real triplet (yellow, dashed), and complex triplet (orange, dot-dashed) models imposing the relations between coefficients shown in Tab. I. The signs of c_H and c_f are fixed in these models, which is why the line segments do not cover the whole plane.

C. Perturbative Unitarity

There are a number of theoretical considerations that can be used to constrain the parameter space of the extended scalar sectors, including requiring the potential to be bounded from below, or requiring the

EW vev to be the deepest of the vacua in the theory.⁵ In this work we focus on theoretical constraints coming from perturbative unitarity [59]. In non-renormalizable theories, such as the SMEFT, scattering amplitudes generally grow with energy leading to a breakdown of unitarity at some critical energy. On the other hand, the extended scalar sectors under consideration are unitarity, and their $2 \rightarrow 2$ scattering amplitudes do not grow with energy at large s . However, the same approach may still be used to examine where the breakdown of perturbation theory occurs. If a certain combination of parameters appearing in a scattering amplitude is too large, the tree level amplitude will not be a good approximation of the full amplitude.

Our approach to finding the unitarity or perturbativity bounds is the same in both cases. We compute all the $2 \rightarrow 2$ scattering amplitudes, $\mathcal{M}_{i \rightarrow f}(s, t)$, in the scalar sector of a given theory, including those containing Goldstone bosons. The set of initial states in the SM and SMEFT with a net electric charge of zero, for example, is $i = \{w^+w^-, zz, hh, hz\}$. The computation is done in the limit that the center-of-mass energy, \sqrt{s} , is much larger than the other scales in the problem. For renormalizable theories this simplifies the scattering amplitudes to a linear combination of quartic couplings. The matrix of $\ell = 0$ partial-wave amplitudes, $(a_0)_{i,f}$, is then computed from these scattering amplitudes

$$(a_0)_{i,f} = \frac{1}{16\pi s} \int_{-s}^0 dt \mathcal{M}_{i \rightarrow f}(s, t). \quad (44)$$

The eigenvalues, a_0 , of this matrix are bounded by the unitarity of the S -matrix

$$|\text{Re}(a_0)| \leq \frac{1}{2}. \quad (45)$$

The unitarity or perturbativity bounds derived in this work ultimately come from (45). For a point in the parameter space to be considered viable, we require that Eq. (45) is satisfied for every eigenvalue for that choice of parameters unless otherwise specified. We consider only tree level contributions, and so our results must be taken as rough estimates near the edge of our viable region. In these regions, the parameters of the potential are becoming strong, and it is possible that loop corrections could provide significant constraints.

We begin by discussing the unitarity bounds on the SMEFT. The Feynman rules for the SMEFT in R_ξ gauge have recently been presented in Ref. [60]. Using the results of [60], and neglecting terms that do not grow with energy, we find the (unique) eigenvalues of the matrix of partial-wave amplitudes for high energy scalar scattering in the SMEFT are

$$a_0 = \frac{s}{32\pi v^2} \{3(c_T + c_H), 3c_T - c_H, -(3c_T + c_H), -c_H\} \quad (46)$$

Since c_T is constrained to be small by the ρ parameter, we can ignore it in determining the critical energy. Our results are in agreement with Ref. [40], which considered a subset of amplitudes (and only c_H). With these approximations, we find the SMEFT will break down at an energy no higher than

$$E_{\text{crit.}} \approx \sqrt{\frac{16\pi}{3c_H}} v \approx \frac{1 \text{ TeV}}{\sqrt{c_H}}. \quad (47)$$

For coefficients, $c_i \sim 1(0.01)$, the EFT is not valid above a scale $E_{\text{crit.}} \sim 1(10)$ TeV. The range of validity of a weakly interacting EFT arising from a high energy scalar sector is thus quite limited [17]. At the scale $E_{\text{crit.}}$, the EFT needs to be matched with the UV complete scalar model, potentially leading to some tension with the lower limits on heavy scalar particles.

We now turn our attention to the perturbativity bounds on the extended scalar sector theories. Using the method described above, typical bounds on the real singlet model with a spontaneously broken Z_2 symmetry are shown in Fig. 2. In the left panel, the contours are labeled with the maximum value of m_H/GeV that is viable at that point. Darker shading indicates viable parameters space for a heavier new scalar. In the right panel, the shaded parameter space is allowed, and going to larger values of

⁵ General bounded from below conditions for models of the type we are interested in can be found in Ref. [58].

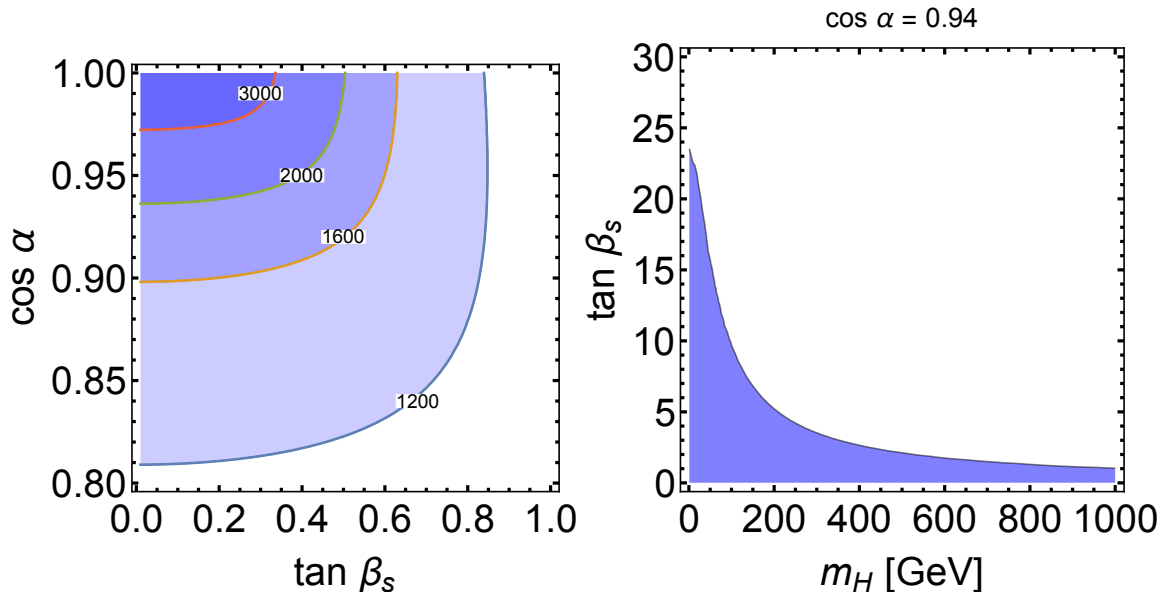


FIG. 2: Perturbativity bounds on the real singlet model with a spontaneously broken Z_2 symmetry. (Left:) The contours are labeled with the maximum value of m_H/GeV that is viable at that point. Going from lighter to darker shading indicates that heavier new scalars are allowed. (Right:) The shaded parameter space is allowed, and going to larger values of $\cos \alpha$ slightly increases the amount of viable parameter space, and darker shading indicates that heavier new scalars are allowed.

$\cos \alpha$ slightly increases the amount of viable parameter space. Considering only the high energy limit of $\mathcal{H}\mathcal{H} \rightarrow \mathcal{H}\mathcal{H}$, perturbative unitarity requires,

$$m_H^2 < \frac{16\pi v^2}{\tan^2 \beta_s}, \quad (48)$$

which explains the general features of the RHS of Fig 2. It is fair to say there is plenty of viable parameter space in this model. The $J = 0$ partial wave for $\mathcal{H}\mathcal{H} \rightarrow \mathcal{H}\mathcal{H}$ scattering can equivalently be expressed in terms of the scalar couplings of Eq. (19),

$$|a_0(s \rightarrow \infty)| = \frac{3|\lambda_\beta|}{2\pi}, \quad (49)$$

making it clear that unitarity violation corresponds to the quartic scalar coupling becoming large.

The real singlet model with an explicitly broken Z_2 symmetry also has a fair amount of viable parameter space. This is illustrated in Fig. 3. Just as in the left panel of Fig. 2, the contours are labeled with the maximum value of m_H that is viable at that point. From Fig. 3 we see that λ_α , which enters into the Wilson coefficient c_6 , is essentially a free parameter. Some of the viable parameter space in Fig. 3 will be ruled out by requiring the potential to be bound from below, $\lambda_\alpha > -2\sqrt{\lambda_\beta}\lambda$, but this does not significantly affect our conclusion. As in the spontaneously broken Z_2 case, perturbative unitarity violation corresponds to large values of the scalar quartic couplings λ_β and the mixed doublet-scalar quartic coupling, λ_α .

The triplet and quartet models exhibit qualitatively similar behavior as far as perturbativity is concerned. The bounds on the real triplet model, with the simplifying assumption that the masses of the heavy Higgs bosons are equal, are shown in Fig. 4. See Fig. 5, Fig. 6, and Fig. 7 for the complex triplet, quartet₁, and quartet₃, respectively. We also assume, for simplicity, the masses of the heavy Higgs bosons are all equal in the complex triplet and quartet₃ models. On the other hand, for the quartet₁ model we take $\bar{m}_{H^+} = \sqrt{2}m_A$, (see Eq. (B18)) and set the masses of the all the non-singly charged, heavy Higgs bosons to be equal. Furthermore, for the quartet₁ model we neglect the eigenvalues from the partial-wave matrices whose initial states had a net electric charge of either zero or one. These are 18×18 and 15×15

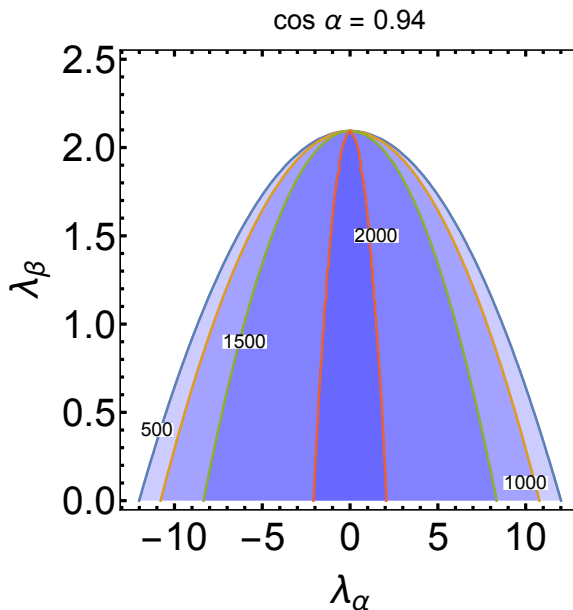


FIG. 3: Perturbativity bounds on the real singlet model with an explicitly broken Z_2 symmetry. Just as in the left panel of Fig. 2, the contours are labeled with the maximum value of m_H/GeV that is viable at that point, and going from lighter to darker shading indicates that heavier new scalars are allowed.

matrices, respectively, and thus are difficult to diagonalize. Explicitly, as an example, the singly charged initial scattering states in the quartet₁ model are

$$i = \{H^{++}H_2^-, H_1^+\mathcal{H}, H_1^+A, H_2^+\mathcal{H}, H_2^+A, H^{++}H_1^-, w^+h, w^+z, H^{++}w^-, H_1^+h, H_1^+z, H_2^+h, H_2^+z, w^+\mathcal{H}, w^+A\}. \quad (50)$$

Similarly, for the quartet₃ model, we did not consider the eigenvalues from the partial-wave matrix whose initial states had a net electric charge of zero, which is a 16×16 matrix.

There are two main points we learn from Figs. 4, 5, 6, and 7. Firstly, unless the ‘heavy’ Higgs bosons are actually somewhat light, $m_H < 200$ GeV, combining the perturbativity bounds with the constraint on $\tan\beta$ coming from the ρ parameter forces $\cos\alpha$ to be much closer to one than experimental measurements would otherwise require. Secondly, for given values of α and β there are upper limits on the masses of the heavy Higgs bosons since no other parameters enter into the quartic couplings. We can use the first point to investigate the second point in more detail.

In the limit $\alpha \approx \beta \approx 0$, which is suggested by Figs. 4, 5, 6, and 7 as the only perturbative region consistent with the ρ parameter, the expressions for the partial wave amplitudes simplify. This allows us to derive fairly simple analytic upper bounds on the masses of the heavy Higgs bosons or on the splittings between different masses in a multiplet. The bounds for the real triplet model with $\alpha \approx \beta \approx 0$ are

$$469 \text{ GeV} > m_H, \quad (51)$$

$$\left(\frac{\beta}{0.03}\right)^2 (11.7 \text{ GeV})^2 > |m_{H^+}^2 - m_H^2|.$$

For numerical purposes we take β to be at its upper limit, $\beta = 0.03$. We also neglected the mass of the 125 GeV Higgs boson in this analysis, which is justified *a posteriori* since both the upper limit on m_H^2 and the mass splitting squared divided by β^2 are quite a bit larger than m_h^2 . Comparable bounds are found in the other models.

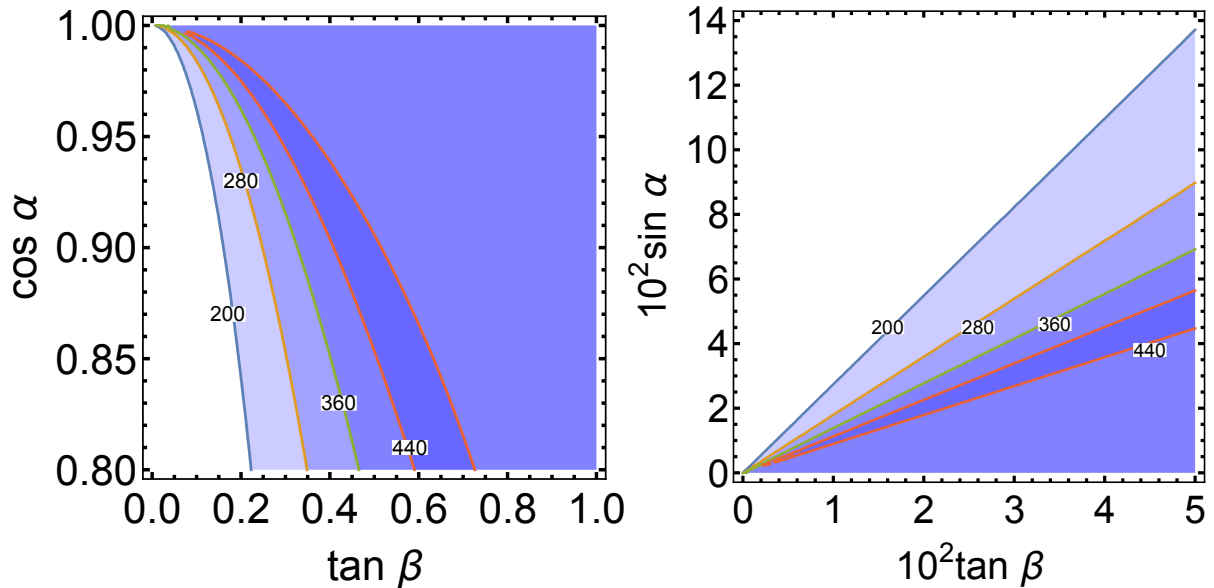


FIG. 4: Perturbativity bounds on the real triplet model. The contours are labeled with the maximum value of m_H/GeV that is viable at that point, with darker shading indicating heavier new scalars are allowed. For simplicity we have set the masses of all the heavy Higgs bosons to be equal. In the absence of relatively light new scalars, combining the perturbativity bounds with the constraint on $\tan \beta$ from the ρ parameter forces $\cos \alpha$ to be much closer to one than experimental measurements would otherwise require.

V. DOUBLE HIGGS PRODUCTION

A. Formalism

Double Higgs boson production in gluon fusion has been computed in Refs. [61, 62]. There have been many studies of double Higgs production using the both EFT approach as well as explicit models [21, 23, 24, 63–67]. The SM rate can be found in Refs. [68, 69]. The rate is dominated by top quark loops, and for simplicity we neglect the b -loops. The SM rate is well below the current experimental limits from ATLAS and CMS [70–73].

Consider a theory with neutral scalars, h and \mathcal{H} , and non-standard scalar cubic couplings and top Yukawa couplings parameterized as follows,

$$\mathcal{L} \supset -\frac{1}{6}\lambda_{hhh}vh^3 - \frac{1}{2}\lambda_{hhH}vh^2\mathcal{H} - y_{ht}\frac{m_t}{v}\bar{t}th - y_{Ht}\frac{m_t}{v}\bar{t}t\mathcal{H}. \quad (52)$$

Expressions for λ_{hhh} and λ_{hhH} in the extended scalar models are given in Appendix B. In the models we consider $y_{ht} = \cos \alpha$ and $y_{Ht} = \sin \alpha$.

The partonic cross section for double Higgs production is [62]

$$\frac{d\hat{\sigma}}{dt} = \frac{G_F^2 \alpha_s^2}{(16\pi)^3} \left(|C_\Delta F_\Delta(s) + C_\square F_\square(s, t)|^2 + |C_\square G_\square(s, t)|^2 \right), \quad (53)$$

where we have included a factor of $\frac{1}{2}$ for identical particles. The coefficients are given by

$$C_\Delta = \sum_{H_i=h,\mathcal{H}} \lambda_{hhH_i} \frac{v^2}{s - m_{H_i}^2 + im_{H_i}\Gamma_{H_i}} y_{H_i t}, \quad C_\square = y_{ht}^2. \quad (54)$$

The form factors simplify considerably in the limit $m_t \rightarrow \infty$ (see [62] for the full expressions),

$$F_\Delta \rightarrow \frac{2}{3} + \mathcal{O}\left(\frac{s}{m_t^2}\right), \quad F_\square \rightarrow -\frac{2}{3} + \mathcal{O}\left(\frac{s}{m_t^2}\right), \quad G_\square \rightarrow \mathcal{O}\left(\frac{s}{m_t^2}\right). \quad (55)$$

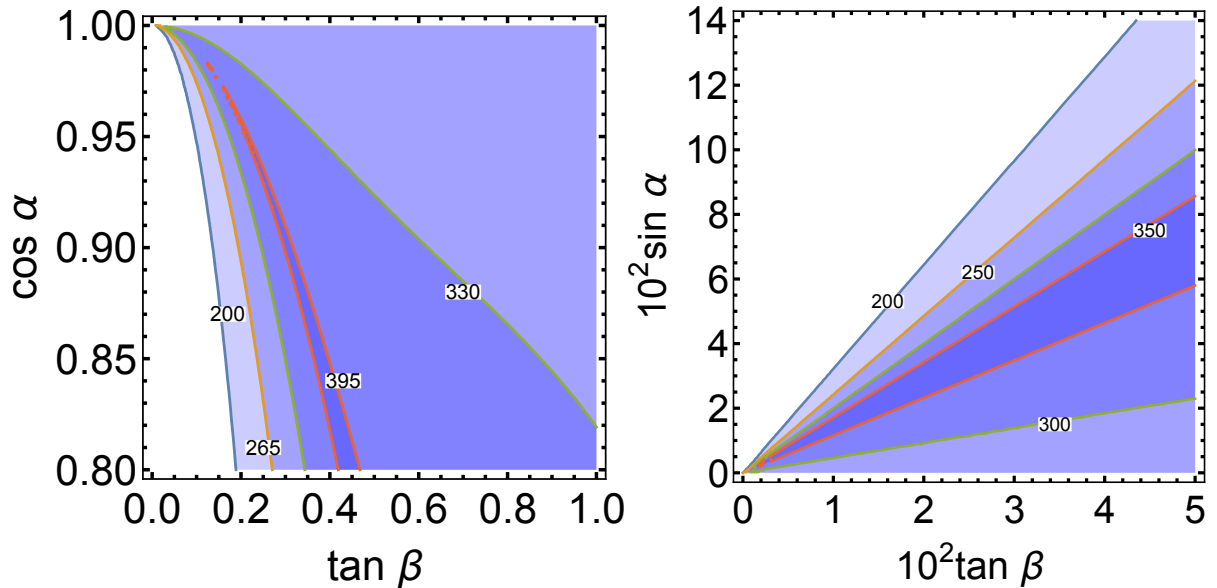


FIG. 5: The same as Fig. 4, but for the complex triplet model.

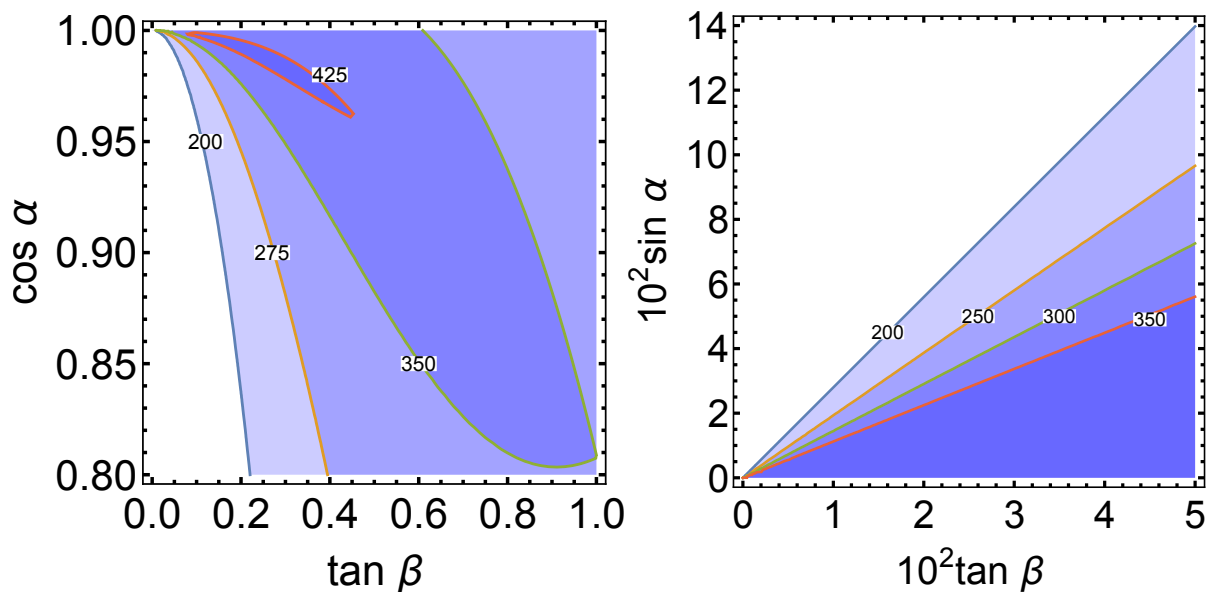


FIG. 6: The same as Fig. 4, but for the quartet₁ model.

In the SMEFT, considering only the top quark, the coefficients appearing in the cross section for double Higgs production are

$$\begin{aligned}
 C_{\Delta} &\approx \frac{3m_h^2}{s - m_h^2 + im_h\Gamma_h} (1 + c_6 - 2c_H - c_t) - (c_H + 3c_t), \\
 C_{\square} &\approx 1 - c_H - 2c_t,
 \end{aligned}
 \tag{56}$$

where we have expanded to linear order in the Wilson coefficients. The second term on the right-hand side of the first line of Eq. (56) comes from the contact interaction $\bar{t}th^2$. Unlike the amplitude, the cross section is not expanded in the Wilson coefficients. This ensures a positive definite cross section.

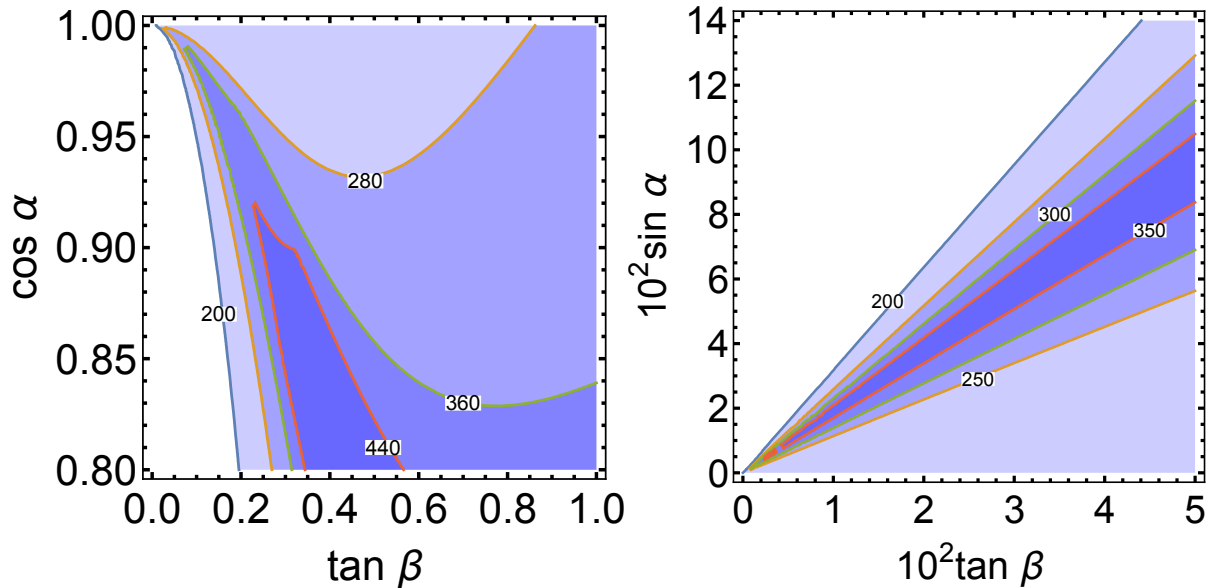


FIG. 7: The same as Fig. 4, but for the quartet₃ model.

The hadronic level invariant mass distribution for double Higgs production is

$$\frac{d\sigma(pp \rightarrow hh)}{dM_{hh}} = \frac{2M_{hh}}{S} ff_{gg} \left(\frac{M_{hh}^2}{S}, M_{hh} \right) \hat{\sigma}(gg \rightarrow hh), \quad (57)$$

with S being the square of the collider center-of-mass energy, $M_{hh}^2 = s$, and ff_{gg} is the gluon luminosity function

$$ff_{gg}(y, \mu_F) = \int_y^1 \frac{dx}{x} f_{g/p}(x, \mu_F) f_{g/p}\left(\frac{y}{x}, \mu_F\right), \quad (58)$$

where $f_{i/p}$ is the proton parton distribution function (PDF) of species i , and μ_F is the factorization scale. The total cross section is obtained by integrating the invariant mass distribution over M_{hh} from $2m_h$ to \sqrt{S} . Unlike the invariant mass distribution, the transverse momentum distribution requires the differential partonic cross section,

$$\frac{d\sigma(pp \rightarrow hh)}{dp_T} = 2p_T \int_{-y^*}^{y^*} dy \frac{2s}{S} ff_{gg} \left(\frac{s}{S}, \frac{\sqrt{s}}{2} \right) \frac{d\hat{\sigma}(gg \rightarrow hh)}{dt}. \quad (59)$$

The limit of integration for the rapidity is

$$y^* = \frac{1}{2} \log \left(\frac{1 + \sqrt{1 - 4(m_h^2 + p_T^2)/S}}{1 - \sqrt{1 - 4(m_h^2 + p_T^2)/S}} \right). \quad (60)$$

Recall that $s = 4(m_h^2 + p_T^2) \cosh^2(y)$ and $t = -p_T^2 - (m_h^2 + p_T^2) \exp(-2y)$.

In the case of a heavy scalar, the p_T distribution is peaked near $m_H^2 = 4(m_h^2 + p_T^2)$. One way to see this is by looking at the p_T distribution in the narrow width approximation (NWA)

$$\frac{d\sigma(pp \rightarrow hh)_{NWA}}{dp_T} = \frac{\alpha_s^2 \lambda_{hhH}^2 y_{Ht}^2}{2048\pi^2 S \Gamma_H} ff_{gg} \left(\frac{m_H^2}{S}, \frac{m_H}{2} \right) \frac{p_T}{\sqrt{m_H^2 - 4(m_h^2 + p_T^2)}} + \mathcal{O}(\Gamma_H^0). \quad (61)$$

The total cross section is finite in the narrow width approximation despite the pole in the p_T distribution

$$\sigma(pp \rightarrow hh)_{NWA} = \frac{\alpha_s^2 \lambda_{hhH}^2 y_{Ht}^2 m_H}{8192\pi^2 S \Gamma_H} \sqrt{1 - \frac{4m_h^2}{m_H^2}} ff_{gg} \left(\frac{m_H^2}{S}, \frac{m_H}{2} \right) + \mathcal{O}(\Gamma_H^0). \quad (62)$$

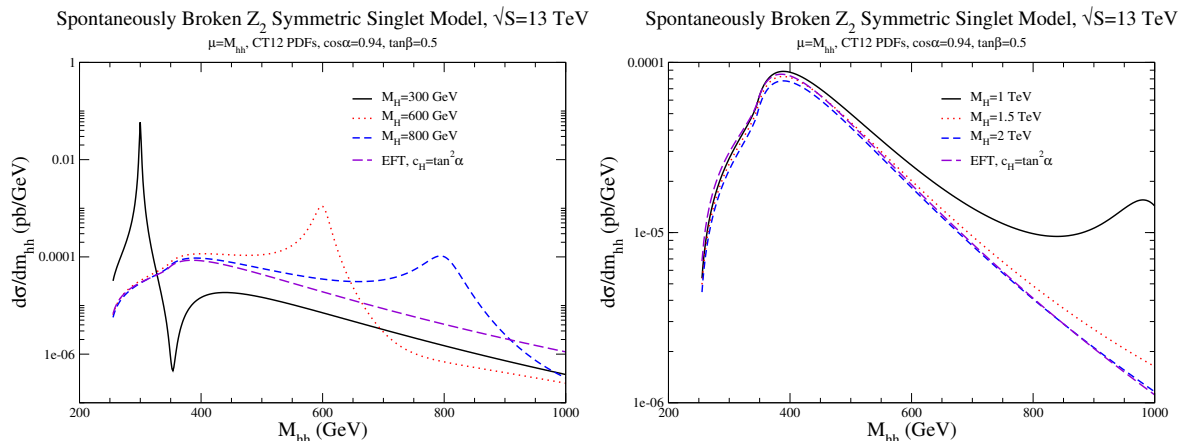


FIG. 8: $d\sigma/dM_{hh}$ in the spontaneously broken Z_2 singlet model compared with the SMEFT predictions.

B. Numerical Results

In this section, we compare predictions for double Higgs production at the LHC in the singlet, triplet, and quartet models with predictions from the dimension-6 SMEFT. We choose input parameters for mixing and masses consistent with restrictions from perturbative unitarity and the ρ parameter. We use CT12NLO [74] PDFs with a scale choice, $\mu_R = \mu_F = \sqrt{s}$. We include the full top quark mass dependence, and neglect the small contribution from the b quark.

1. Singlet Model with spontaneously broken Z_2 symmetry

In the SMEFT for the singlet model with a spontaneously broken Z_2 symmetry, only c_H is non-zero, and we employ the large mass limit for the SMEFT results, $c_H \sim \tan^2 \alpha$, in our plots. In this model, the Z_2 symmetry imposes $c_6 = 0$ [3–5].

The left-hand sides of Fig. 8 and Fig. 9 show the invariant mass distributions for the spontaneously broken Z_2 singlet model for heavy Higgs masses of $m_H = 300, 600$ and 800 GeV for $\sqrt{S} = 13$ and 100 TeV. The resonance peaks and interference patterns are clearly observed. The results in the SMEFT are also shown. For $m_H = 600$ and $m_H = 800$ GeV, the SMEFT is a good approximation to the invariant mass distribution below around 400 GeV at both $\sqrt{S} = 13$ and 100 TeV. Heavier masses are shown on the right-hand sides of Fig. 8 and Fig. 9. Below $M_{hh} \sim m_H/2$ the agreement between the singlet model results and the SMEFT limit is excellent. By the time m_H reaches 2 TeV, the SMEFT almost exactly reproduces the full model results.

The p_T distributions for the spontaneously broken Z_2 symmetric model are shown in Fig. 10. For $m_H \sim 1.5$ TeV, the agreement below the resonance peak between the exact and SMEFT results is good below about $p_T \sim 400$ GeV, while for $m_H = 2$ TeV, the agreement is within a factor of 2 even at $p_T = 1$ TeV.

2. Singlet Model with explicitly broken Z_2 Symmetry

The singlet model with explicit breaking of the Z_2 symmetry is described by 6 parameters that we fix to be $v, m_h, m_H, \alpha, \lambda_\alpha$, and m_2 . We take $\cos \alpha = 0.94$, $\lambda_\alpha = 0.1$ ($\lambda_\alpha = 1$), and $m_2 = v$ for our numerical study. These parameters are chosen to obey all constraints from unitarity and the ρ parameter. In Fig. 11, we show the M_{hh} in the explicitly broken Z_2 singlet model and compare it with the SMEFT predictions. The new feature of this model is that c_6 is no longer forced to be zero and can be tuned by adjusting λ_α . We see fairly good agreement between the full theory and the SMEFT for $m_H \sim 2$ TeV.

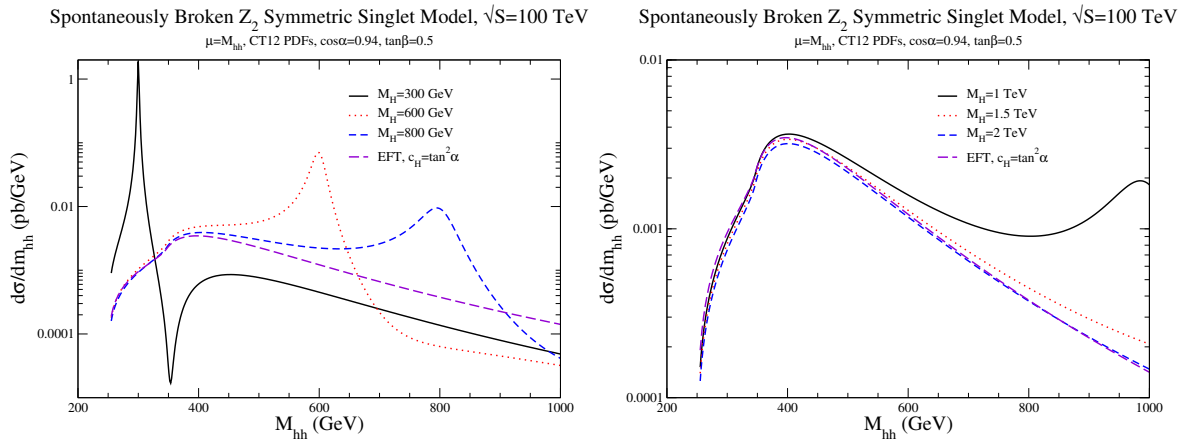


FIG. 9: $d\sigma/dM_{hh}$ in the spontaneously broken Z_2 singlet model compared with the SMEFT predictions.

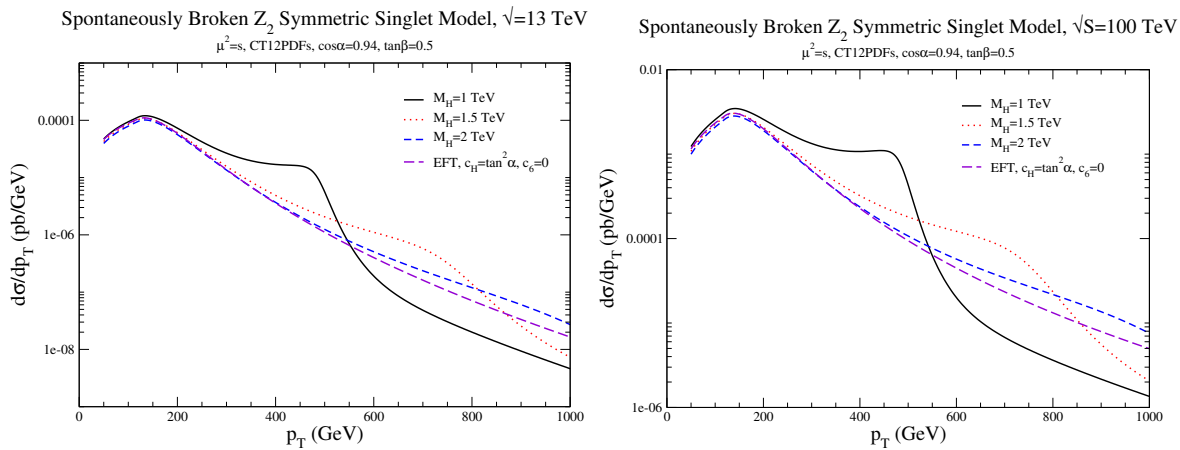


FIG. 10: $d\sigma/dp_T$ in the spontaneously broken Z_2 singlet model compared with the SMEFT predictions.

3. Triplet Models

The triplet model is highly restricted by the experimental limit on the ρ parameter and when parameters are chosen so as to be consistent with the ρ parameter and perturbative unitarity, the mixing angle α is forced to be so small as to make the $gg \rightarrow hh$ cross section indistinguishable from the SM result. This is a case where the new physics is not probed by either single or double Higgs production.

4. Quartet Models

From the previous sections, we see that the limit on the ρ parameter requires $\beta < 0.033$ for the quartet₁ model and $\beta < 0.010$ for the quartet₃ model. For small $\tan\beta$ and small mixing α , perturbative unitarity allows small regions of parameter space where the scalar masses are fine tuned. The allowed scalar masses are electroweak scale, so the SMEFT is not applicable. In Fig 12, we compare the tri-linear Higgs coupling to the SM coupling for allowed parameters in the quartet₁ model. For $\tan\beta \rightarrow 0$ and $\sin\alpha \rightarrow 0$, the SM is recovered, although $\cos\alpha = 0.94$ gives significant deviations in the hhh coupling from the SM result. When the hhh coupling is non-SM like, the SM cancellation between the triangle and box contributions to $gg \rightarrow hh$ is spoiled, and the results differ significantly from the SM. This is clear in the $\cos\alpha = 0.94$ curve on the RHS of Fig. 12.

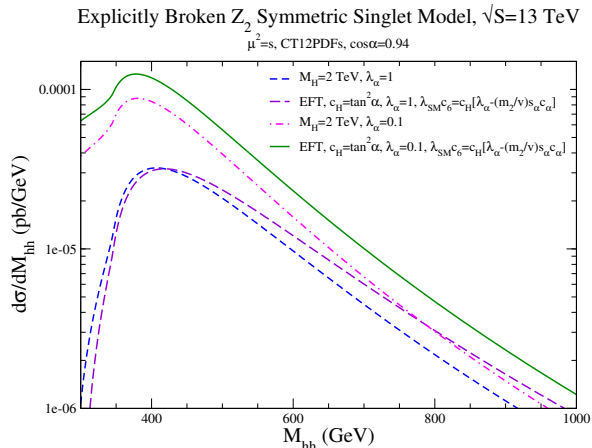


FIG. 11: $d\sigma/dM_{hh}$ in the explicitly broken Z_2 singlet model compared with the SMEFT predictions.

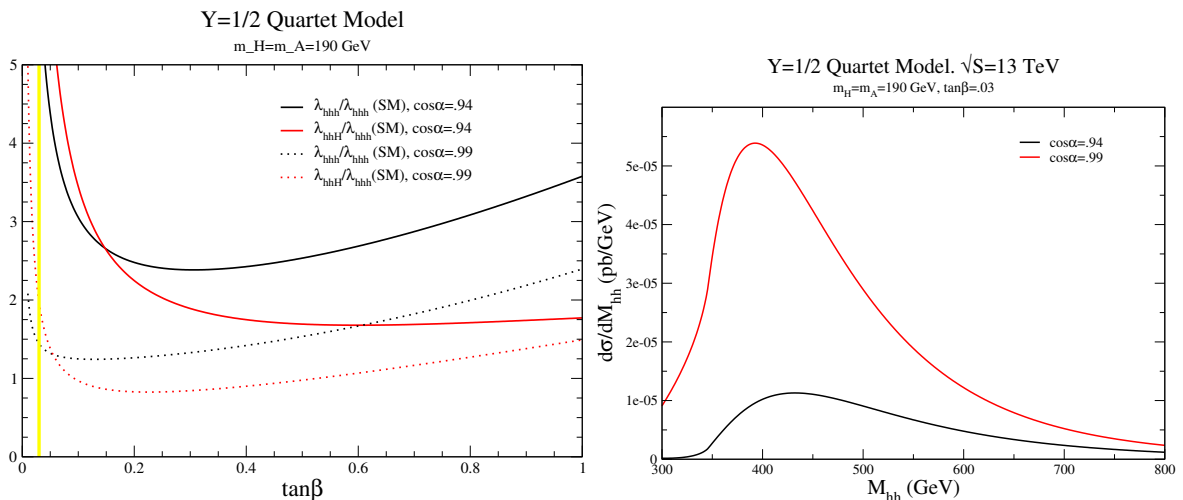


FIG. 12: Tri-linear Higgs couplings in the $Y = \frac{1}{2}$ quartet model, normalized to the SM result (LHS). The vertical yellow line is the largest value of $\tan\beta = 0.03$ allowed by perturbative unitarity for the chosen masses. The RHS shows the invariant mass distribution for 2 choices for the neutral mixing angle, α .

VI. CONCLUSIONS

We have considered modifications of the SM with additional $SU(2)_L$ Higgs singlets, triplets, and quartets and computed their contributions to SMEFT coefficients in the limits that the new scalars are heavy. The coefficients show a characteristic pattern in the heavy mass limit, shown in Tab. I. A feature of the extended scalar models considered here is that they generate only a subset of the possible SMEFT operators. A fit to these operators from single Higgs production (Fig. 1) shows that the data can not yet distinguish between the extended scalar sectors considered here, although the sign of the c_H is a generic signature of the UV scalar multiplet.

The parameters of the extended sectors are restricted by measurements of the ρ parameter (see Tab. III) and perturbative unitarity. In the triplet and quartet models, the ρ parameter limits typically force $\tan\beta$ to be small, while in all models, the requirement of perturbative unitarity puts an upper limit on the heavy neutral scalar, m_H , for a given value of $\tan\beta$. We have performed a consistent dimension-6 matching of the scalar models to the EFT, with the exception of the quartet model, where we have included the first non-zero tree level contribution to the ρ parameter, which arises at dimension-8. A complete dimension-8 study of the quartet model would be of interest, but beyond the scope of this work.

Operator	Relation to [36] References: Coefficients, \bar{C}_i :	Operators, O_i			
		[36] C_i	[10] a_i	[35] $\frac{c_i}{v^2}$	[3] c_i
$ D^2 H ^2$	$ EoM ^2$				\mathcal{O}_D
$(H^\dagger H) (D_\mu H^\dagger D^\mu H)$	$\frac{1}{2} Q_{H\Box} - \frac{1}{2} (H^\dagger H) (H^\dagger EoM + \text{h.c.})$		O_2		\mathcal{O}_R
$(\partial_\mu (H^\dagger H))^2$	$-Q_{H\Box}$			$2O_H$	$2\mathcal{O}_H$
$ H^\dagger \overleftrightarrow{D}_\mu H ^2$	$-Q_{H\Box} - 4Q_{HD}$			$2O_T$	$2\mathcal{O}_T$
$(H^\dagger H) \Box (H^\dagger H)$		$Q_{H\Box}$	$2O_1$		
$ H^\dagger D_\mu H ^2$		Q_{HD}	O_T		
$(H^\dagger H)^3$		Q_H	\checkmark	$\frac{1}{\lambda} O_6$	\mathcal{O}_6

TABLE V: Summary of dimension-6 operators involving H and D_μ , including relations amongst the operators and the notation in the literature. The effective Lagrangian in each basis is $L = \Sigma_i \bar{C}_i O_i$.

There are regions of parameter space in the triplet model that are consistent with limits from the ρ parameter, perturbative unitarity, and single Higgs production. In these models, the mixing between the two neutral Higgs bosons is forced to be so small that both single and double Higgs production look SM-like. These models must be probed by searches for the charged scalars, which are required by perturbative unitarity to be rather light. The quartet models examined here have small regions of scalar masses simultaneously allowed by the ρ parameter and perturbative unitarity limits. In both the triplet and quartet models, however, the scalars are typically forced to be electroweak scale making the SMEFT not applicable.

The most interesting model considered here is the singlet model. We have considered models with a spontaneously broken and an explicitly broken Z_2 symmetry. Limits from perturbative unitarity require $\tan \beta_s < 1$ in the spontaneously broken model, but allow for a TeV scale neutral Higgs boson. Comparisons of the invariant mass and p_T distributions from double Higgs production in the singlet models show that for $m_H \gtrsim 2$ TeV, the agreement between the exact calculations and the SMEFT results is excellent.

Acknowledgments

This work was supported by the United States Department of Energy under Grant Contract DE-SC0012704.

Appendix A: EFT Details

To help set the notation, consider the scalar potential of the SM

$$V_{SM} = -\mu^2 H^\dagger H + \lambda (H^\dagger H)^2, \quad (\text{A1})$$

where $H^T = (w^+, (v + h + iz)/\sqrt{2})$ with w^\pm and z being the Goldstone bosons, and h is the physical Higgs scalar. The vev of the Higgs fields is set by minimizing the potential (A1), $v = \mu/\sqrt{\lambda}$. The tree level mass for the Higgs boson is given by $m_h^2 = 2\lambda v^2$. Finally, the equation of motion for the Higgs in the SM is [37, 75]

$$D^2 H_k = \lambda v^2 H_k + 2\lambda (H^\dagger H) H_k - \bar{q}^j y_u^\dagger u \epsilon_{jk} + \bar{d} y_d q_k + \bar{e} y_e \ell_k \equiv EoM, \quad (\text{A2})$$

where j, k are $SU(2)$ indices, the flavor indices are implicit, and $\epsilon = \epsilon_{[jk]}$ with $\epsilon_{12} = +1$.

Table V summarizes the possible dimension-6 operators involving H and D_μ , the relations amongst these operators, and how they are referred to in the literature [3, 10, 35, 36]. It is straightforward to switch between operator bases, and convenient tables are given in Refs. [35, 76].

Redundant operators may appear in intermediate steps of calculations. An example of such an operator is $O_R = H^\dagger H (D_\mu H)^\dagger (D^\mu H)$ with coefficient c_R/v^2 . To extract the coefficients of the $D^2 H^4$ operators we

follow the approach of [10], which considers the following scattering processes evaluated at the matching scale

$$\begin{aligned}\mathcal{M}(H_1(p)H_2(0) \rightarrow H_1(p)H_2(0)) &= c_R \frac{p^2}{v^2}, \\ \mathcal{M}(H_1(p)H_2(0) \rightarrow H_1(0)H_2(p)) &= (c_H - c_T) \frac{p^2}{v^2}, \\ \mathcal{M}(H_1(p)H_2(-p) \rightarrow H_1(0)H_2(0)) &= (c_H + c_T) \frac{p^2}{v^2}.\end{aligned}\tag{A3}$$

The subscripts in the above equations indicate the component of the Higgs doublet. The operator \mathcal{O}_R can be removed with the following field definition [40, 77]

$$H \rightarrow H - \frac{c_R}{2v^2} (H^\dagger H) H.\tag{A4}$$

This field definition leads to contributions to the non-redundant operators

$$c_H \rightarrow c_H - c_R, \quad c_f \rightarrow c_f + c_R/2.\tag{A5}$$

As previously mentioned, the kinetic energy for the Higgs boson, h , in Eq. (1) is not canonically normalized. This can be remedied by a simply rescaling [16, 39]

$$h \rightarrow h/\sqrt{1 + c_H}.\tag{A6}$$

Alternatively, a field redefinition can be made to correctly normalize the kinetic energy and eliminate the derivative interactions [40, 41], Eq. (6). We stress that the two approaches yield equivalent results for physical observables, as expected. Using (6) the Lagrangian now takes the form of Eq. (7). For example, both approaches lead to the following amplitude for Higgs-Higgs scattering

$$\begin{aligned}\mathcal{M}(hh \rightarrow hh) &= -\frac{3m_h^2}{2v^2} \left[2 + 12c_6 + \frac{50}{3}c_H \right. \\ &\quad \left. + 3(1 + 2c_6 - 3c_H) \left(\frac{m_h^2}{s - m_h^2} + \frac{m_h^2}{t - m_h^2} + \frac{m_h^2}{u - m_h^2} \right) \right].\end{aligned}\tag{A7}$$

Appendix B: Scalar Model Details

In this Appendix we give some additional details of the models considered in this work. The mixing angles analogous to α in (12) in the CP -odd and charged Higgs sectors are functions of β , and are denoted δ and γ , respectively.⁶ Additionally, we will sometimes express the sine, cosine, or tangent of an angle θ as s_θ , c_θ , or t_θ , respectively. Furthermore, we will sometimes use the following notation,

$$\lambda'_i = \lambda_i v^2 / \rho, \quad m'_i = m_i v / \rho,\tag{B1}$$

with ρ given in Tab. III for each model.

1. Real Singlet with Explicit Z_2 Breaking

It is straightforward to compute the dimension-6 operators [3]

$$c_6 \lambda_{SM} = \frac{m_1^2 v^2}{M^4} \left(\lambda_\alpha - \frac{m_1 m_2}{M^2} \right), \quad c_H = \frac{m_1^2 v^2}{M^4}, \quad c_T = c_f = 0.\tag{B2}$$

⁶ There are three singly charged scalars in the quartet₁ model, and thus the diagonalization is more complicated in this case.

There are also shifts in the parameters of the renormalizable Lagrangian, for example, $\Delta\lambda = -m_1^2/2M^2$. However these shifts are unphysical, and can simply be reabsorbed into the definition of the original parameters in the effective theory. We have checked by explicit computation that the matching is the same when starting either from the unbroken or broken phase of the full theory.

Now consider the masses and mixings in the full theory. The relations between the masses, mixing angle α , and the Lagrangian parameters in the full theory (see (16)) are

$$\begin{aligned} 4\lambda v^2 &= m_h^2 + m_H^2 + (m_h^2 - m_H^2) \cos 2\alpha, \\ 2M^2 &= m_H^2 + m_h^2 + (m_H^2 - m_h^2) \cos 2\alpha, \\ 2m_1 v &= (m_H^2 - m_h^2) \sin 2\alpha. \end{aligned} \quad (\text{B3})$$

Lastly, the couplings in the full theory that are relevant for double Higgs production are

$$\begin{aligned} \lambda_{hhh} v^2/3 &= m_h^2 \cos^3 \alpha + 2v \sin^2 \alpha (\lambda_\alpha v \cos \alpha - m_2 \sin \alpha), \\ 2\lambda_{hhH} v^2/\sin \alpha &= (2m_h^2 + m_H^2) \cos^2 \alpha - 2v (\lambda_\alpha v (1 + 3 \cos 2\alpha) - 3m_2 \sin 2\alpha). \end{aligned} \quad (\text{B4})$$

2. Real Singlet with Spontaneous Z_2 Breaking

The only operator generated in this case is [5]

$$c_H = \left(\frac{\lambda_\alpha v}{4\lambda_\beta v_\phi} \right)^2. \quad (\text{B5})$$

In terms of mass eigenstates the quartic couplings in (21) are

$$\begin{aligned} 4\lambda v^2 &= m_h^2 + m_H^2 + (m_h^2 - m_H^2) \cos 2\alpha, \\ 4\lambda_\alpha v_\phi v &= (m_H^2 - m_h^2) \sin 2\alpha, \\ 16\lambda_\beta v_\phi^2 &= m_H^2 + m_h^2 + (m_H^2 - m_h^2) \cos 2\alpha, \end{aligned} \quad (\text{B6})$$

with α the same as in Eq. (12). Interestingly, in the case of spontaneous Z_2 breaking, c_H has the exact same form as (17) when written in terms of the physical masses and mixing angle.

The couplings relevant for double Higgs production are somewhat simpler in this case

$$\begin{aligned} \lambda_{hhh} &= \frac{3m_h^2}{v^2} \left(\cos^3 \alpha - \frac{v}{v_\phi} \sin 3\alpha \right), \\ \lambda_{hhH} &= \frac{2m_h^2 + m_H^2}{2v^2} \sin 2\alpha \left(\cos \alpha + \frac{v}{v_\phi} \sin \alpha \right). \end{aligned} \quad (\text{B7})$$

3. Real Triplet

The coefficients of the dimension-6 operators are [3, 10],

$$c_H = -\frac{m_1^2 v^2}{2M^4}, \quad c_T = -\frac{c_H}{2}, \quad c_6 \lambda_{SM} = -\frac{c_H}{2} \lambda_\alpha, \quad c_f = -\frac{c_H}{2}. \quad (\text{B8})$$

Minimizing the potential ($V = (23) + V_{SM}$) yields the constraints

$$\begin{aligned} 4\mu^2 &= 4\lambda v^2 c_\beta^2 - m_1 v s_\beta + \lambda_\alpha v^2 s_\beta^2, \\ 2M^2 v s_\beta &= m_1 v^2 c_\beta^2 - 2\lambda_\alpha v^3 c_\beta^2 s_\beta - 2\lambda_\beta v^3 s_\beta^3. \end{aligned} \quad (\text{B9})$$

The mixing angle in the charged sector is $\gamma = \beta$. The Lagrangian parameters can be traded for the masses of the particles and the mixing angles

$$\begin{aligned} m_1 v &= 2m_{H^+}^2 \sin \beta, \\ 4\lambda' &= m_h^2 + m_H^2 + (m_h^2 - m_H^2) \cos 2\alpha, \\ \lambda_\alpha v^2 &= m_{H^+}^2 + (m_H^2 - m_h^2) \csc 2\beta \sin 2\alpha, \\ 4\lambda_\beta v^2 &= 2m_{H^+}^2 + (m_h^2 + m_H^2 - 2m_{H^+}^2 + (m_H^2 - m_h^2) \cos 2\alpha) \csc^2 \beta. \end{aligned} \quad (\text{B10})$$

The cubic couplings relevant for double Higgs production are

$$\begin{aligned}\lambda_{hhh}v^2 &= 3m_h^2 \left(c_\alpha^3 c_\beta^{-1} - 2s_\alpha^3 s_\beta^{-1} \right) + 6m_{H^+}^2 s_\alpha^2 t_\beta^{-1} s_{\alpha+\beta}, \\ \lambda_{hhH}v^2 &= (2m_h^2 + m_H^2) s_\alpha c_\alpha \left(c_\alpha c_\beta^{-1} + 2s_\alpha s_\beta^{-1} \right) - m_{H^+}^2 s_\alpha t_\beta^{-1} (s_\beta + 3s_{2\alpha+\beta}).\end{aligned}\quad (\text{B11})$$

4. Complex Triplet

The coefficients of the dimension-6 operators are [4, 10]

$$c_H = -\frac{m_1^2 v^2}{2M^4}, \quad c_T = c_H, \quad c_6 \lambda_{SM} = c_H \left(\frac{\lambda_{\alpha 2}}{2} - \lambda_{\alpha 1} \right), \quad c_f = -c_H. \quad (\text{B12})$$

Minimizing the potential ($V = (25) + V_{SM}$) yields the constraints

$$\begin{aligned}8\mu^2 &= 8\lambda v^2 c_\beta^2 + 4\sqrt{2}m_1 v s_\beta + (2\lambda_{\alpha 1} - \lambda_{\alpha 2}) v^2 s_\beta^2, \\ -2M^2 s_\beta &= 2\sqrt{2}m_1 v c_\beta^2 + (2\lambda_{\alpha 1} - \lambda_{\alpha 2}) v^2 c_\beta^2 s_\beta - 2(\lambda_{\beta 1} + \lambda_{\beta 2}) v^2 s_\beta^3.\end{aligned}\quad (\text{B13})$$

The CP -odd and charged Higgs mixing angles are $\tan 2\delta = (2\sqrt{2}\sin 2\beta)/(1 - 3\cos 2\beta)$ and $\gamma = -\beta$, respectively. In terms of the physical masses and CP -even mixing angle, the Lagrangian interaction parameters are

$$\begin{aligned}-m'_1 &= \sqrt{2}m_A^2 \sin \beta, \\ 4\lambda v^2 \cos^2 \beta &= m_h^2 + m_H^2 + (m_h^2 - m_H^2) \cos 2\alpha, \\ \lambda_{\alpha 1} v^2 &= 2m_{H^+}^2 + \sqrt{2}(m_H^2 - m_h^2) \csc 2\beta \sin 2\alpha, \\ \lambda'_{\alpha 2} &= 2m_{H^+}^2 (3 - \cos 2\beta) - 4m_A^2, \\ 2\lambda_{\beta 1} v^2 &= 4m_{H^+}^2 + (m_h^2 + m_H^2 - 4m_{H^+}^2 + 2m_{H^{++}}^2 + (m_H^2 - m_h^2) \cos 2\alpha) \csc^2 \beta, \\ -\lambda'_{\beta 2} &= 2m_{H^+}^2 \sin^2 \beta - m_A^2 + m_{H^{++}}^2 + (m_A^2 - 2m_{H^+}^2 + m_{H^{++}}^2) \csc^2 \beta.\end{aligned}\quad (\text{B14})$$

The scalar cubic couplings are

$$\begin{aligned}\frac{2}{3}\lambda'_{hhh} &= (2m_A^2 - m_h^2 - (m_h^2 + 2m_A^2) c_{2\alpha}) c_\alpha c_\beta + 4m_h^2 c_\alpha^3 c_\beta^{-1} \\ &\quad + \sqrt{2}(m_A^2 - 3m_h^2 + (m_h^2 + m_A^2) c_{2\beta}) s_\alpha^3 s_\beta^{-1}, \\ 2\lambda'_{hhH} &= (2m_h^2 + m_H^2) c_\alpha s_\alpha (3 - c_{2\beta}) (c_\alpha c_\beta^{-1} + \sqrt{2}s_\beta^{-1} s_\alpha) \\ &\quad - m_A^2 c_\beta \left(s_\alpha (3\sqrt{2}t_\beta^{-1} s_{2\alpha} - 1) + 3s_{3\alpha} \right).\end{aligned}\quad (\text{B15})$$

5. Quartet₁

The potential ($V = (27) + (28) + V_{SM}$) minimization conditions are

$$\begin{aligned}\frac{\mu^2}{v^2} &= \lambda c_\beta^2 - \frac{\sqrt{21}}{14} \lambda_1 c_\beta s_\beta + \frac{1}{42} (3\lambda_{\alpha 1} + 2\lambda_{\alpha 2}) s_\beta^2, \\ \frac{M^2}{v^2} s_\beta &= \frac{\sqrt{21}}{6} \lambda_1 c_\beta^3 - \frac{1}{6} (3\lambda_{\alpha 1} + 2\lambda_{\alpha 2}) c_\beta^2 s_\beta - \frac{1}{63} (9\lambda_{\beta 1} + 5\lambda_{\beta 2}) s_\beta^3.\end{aligned}\quad (\text{B16})$$

The rotation to the mass basis is most complicated in this case as there are three singly charged scalars. The charged mass matrix is

$$\begin{aligned}\mathcal{M}_{H^+} &= \frac{v^2 c_\beta^2}{42} \\ &\times \begin{pmatrix} t_\beta (7\sqrt{21}\lambda_1 - \lambda_{\alpha 2} t_\beta) & 2(\sqrt{7}\lambda_{\alpha 2} t_\beta - 7\sqrt{3}\lambda_1) & 21\lambda_1 + \sqrt{21}\lambda_{\alpha 2} t_\beta \\ 2(\sqrt{7}\lambda_{\alpha 2} t_\beta - 7\sqrt{3}\lambda_1) & 7\sqrt{21}\lambda_1 t_\beta^{-1} + 2\lambda_{\beta 2} t_\beta^2 - 7\lambda_{\alpha 2} & \frac{4\sqrt{3}}{3}\lambda_{\beta 2} t_\beta^2 \\ 21\lambda_1 + \sqrt{21}\lambda_{\alpha 2} t_\beta & \frac{4\sqrt{3}}{3}\lambda_{\beta 2} t_\beta^2 & 7\sqrt{21}\lambda_1 t_\beta^{-1} + \frac{8}{3}\lambda_{\beta 2} t_\beta^2 + 7\lambda_{\alpha 2} \end{pmatrix}.\end{aligned}\quad (\text{B17})$$

The determinant of \mathcal{M}_{H^+} is zero, as required by having a massless Goldstone boson. This also allows us to write the masses of the charged Higgs bosons, $m_{H_{1,2}^+}$, as

$$\begin{aligned} 2m_{H_{1,2}^+} &= \bar{m}_{H^+}^2 \mp \Delta m_{H^+}^2, \\ \bar{m}_{H^+}^2 &= \text{Tr}(\mathcal{M}_{H^+}), \\ \Delta m_{H^+}^4 &= 2 \text{Tr}(\mathcal{M}_{H^+}^2) - \text{Tr}(\mathcal{M}_{H^+})^2. \end{aligned} \quad (\text{B18})$$

As physical parameters we choose the masses of the CP -even Higgs bosons, their mixing angle, the mass of the CP -odd Higgs boson, the mass of the doubly charged Higgs boson, and finally \bar{m}_{H^+} , which is twice the average of the mass squared of the singly charged Higgs bosons. In terms of these quantities, the Lagrangian parameters are

$$\begin{aligned} 28\lambda' &= 6(m_h^2 + m_H^2 - m_A^2) + (m_h^2 + m_H^2 + 6m_A^2)c_\beta^{-2} + (m_h^2 - m_H^2)c_{2\alpha}(6 + c_\beta^{-2}), \\ \sqrt{7}\lambda'_1 &= 2\sqrt{3}m_A^2 t_\beta, \\ 14\lambda'_{\alpha 1} &= \frac{1}{25 + 24c_{2\beta}} [112(7m_{H^{++}}^2 + 2\bar{m}_{H^+}^2 - 2m_A^2) + 42(3m_A^2 + 14m_{H^{++}}^2 + 4\bar{m}_{H^+}^2)c_{2\beta} \\ &\quad - \sqrt{7}(m_h^2 - m_H^2)(136 + 171c_{2\beta} + 36c_{4\beta})s_\beta^{-1}c_\beta^{-1}s_{2\alpha}], \\ \lambda'_{\alpha 2} &= \frac{3}{1 + 49t_\beta^{-2}} [6(7m_{H^{++}}^2 + 2\bar{m}_{H^+}^2) - 63m_A^2 + 7(11m_A^2 - 7m_{H^{++}}^2 - 2\bar{m}_{H^+}^2)s_\beta^{-2}], \\ 4\lambda'_{\beta 1} &= \frac{1}{25 + 24c_{2\beta}} [40(m_{H^{++}}^2 + 35\bar{m}_{H^+}^2) - 1463m_A^2 - 486(m_h^2 + m_H^2) \\ &\quad - 3(63m_A^2 + 48(m_h^2 + m_H^2) - 10(m_{H^{++}}^2 + 14\bar{m}_{H^+}^2))c_{2\beta} \\ &\quad + 49(26m_A^2 + 7(m_h^2 + m_H^2) - 20\bar{m}_{H^+}^2)s_\beta^{-2} \\ &\quad + (m_h^2 - m_H^2)c_{2\alpha}(486 + 144c_{2\beta} - 343s_\beta^{-2})], \\ 4\lambda'_{\beta 2} &= \frac{9}{25 + 24c_{2\beta}} [497m_A^2 - 8(m_{H^{++}}^2 + 35\bar{m}_{H^+}^2) \\ &\quad + 3(35m_A^2 - 2(m_{H^{++}}^2 + 14\bar{m}_{H^+}^2))c_{2\beta} + 196(\bar{m}_{H^+}^2 - 2m_A^2)s_\beta^{-2}]. \end{aligned} \quad (\text{B19})$$

For generic parameters, the splitting between the masses of the singly charged Higgs bosons is

$$\begin{aligned} \frac{\Delta m_{H^+}^4}{\bar{m}_{H^+}^4} &= 1 + \frac{7}{25 + 24c_{2\beta}} \frac{m_{H^{++}}^2}{\bar{m}_{H^+}^2} \left(2 + \frac{7m_{H^{++}}^2}{4\bar{m}_{H^+}^2} \right) \\ &\quad - \frac{1470c_\beta^2}{(4 + 3c_{2\beta})(25 + 24c_{2\beta})} \frac{m_A^2}{\bar{m}_{H^+}^2} \left(1 + \frac{3}{5} \frac{m_{H^{++}}}{\bar{m}_{H^+}} \right) + \frac{147c_\beta^2(155 + 27c_{2\beta})}{2(4 + 3c_{2\beta})^2(25 + 24c_{2\beta})} \frac{m_A^4}{\bar{m}_{H^+}^4}. \end{aligned} \quad (\text{B20})$$

We caution that Eq. (B20) will not work in certain special cases, such as when there are degeneracies in some of the mass parameters. Note however that Eq. (B18) will always be correct. Lastly, the cubic couplings are

$$\begin{aligned} \frac{7}{3}\lambda'_{hhh} &= m_h^2(4 + 3c_{2\beta})c_\beta^{-1}(c_\alpha^3 - \sqrt{7}t_\beta^{-1}s_\alpha^3) \\ &\quad + m_A^2(c_\alpha(10 - 11c_{2\alpha})c_\beta + c_\alpha^3c_\beta^{-1} + \sqrt{7}s_\alpha(5c_{2\alpha} - 2 + 7s_\beta^{-2}s_\alpha^2)s_\beta), \\ 14\lambda'_{hhH} &= (2m_h^2 + m_H^2)(4 + 3c_{2\beta})(c_\alpha c_\beta^{-1} + \sqrt{7}s_\alpha s_\beta^{-1})s_{2\alpha} \\ &\quad + 3m_A^2(s_\alpha(2c_\alpha^2c_\beta^{-1} - 7\sqrt{7}s_\beta^{-1}s_{2\alpha}) + c_\beta(3s_\alpha - 11s_{3\alpha}) + \sqrt{7}(3c_\alpha - 5c_{3\alpha})s_\beta). \end{aligned} \quad (\text{B21})$$

6. Quartet₃

The potential ($V = (27) + (32) + V_{\text{SM}}$) minimization conditions are

$$\begin{aligned} 6\frac{\mu^2}{v^2} &= 6\lambda c_\beta^2 - 3\sqrt{3}\lambda_1 c_\beta s_\beta + (\lambda_{\alpha 1} + \lambda_{\alpha 2}) s_\beta^2, \\ 6\sqrt{3}\frac{M^2}{v^2} s_\beta^{-2} &= 9\lambda_1 t_\beta^{-3} - 3\sqrt{3}(\lambda_{\alpha 1} + \lambda_{\alpha 2}) t_\beta^{-2} - 2\sqrt{3}(\lambda_{\beta 1} + \lambda_{\beta 2}). \end{aligned} \quad (\text{B22})$$

The six quartic couplings can be traded for m_h , m_H , m_A , m_{H^+} , $m_{H^{++}}$, and α , the mixing angle between the CP -even Higgs bosons. The mixing angle analogous to α in (12) for the charged states is $\gamma = -\beta$, and similarly for the CP -odd states we have $\tan \delta = -\sqrt{3} \tan \beta$. The quartic couplings are

$$\begin{aligned} 4\lambda' &= (2m_A^2 + 3(m_h^2 + m_H^2)) c_\beta^{-2} - 2(m_A^2 + m_h^2 + m_H^2) + (m_h^2 - m_H^2) c_{2\alpha} (3c_\beta^{-2} - 2), \\ \sqrt{3}\lambda'_1 &= 2m_A^2 t_\beta, \\ 2\lambda'_{\alpha 1} &= 6(2m_{H^+}^2 (2 - c_{2\beta}) - m_A^2) + \sqrt{3}(m_H^2 - m_h^2) (2 - c_{2\beta}) s_\beta^{-1} c_\beta^{-1} s_{2\alpha}, \\ \lambda'_{\alpha 2} &= 6(m_A^2 - m_{H^+}^2 (2 - c_{2\beta})), \\ \frac{4}{3}\lambda'_{\beta 1} &= 2(m_h^2 + m_H^2 - 2m_A^2 + 6m_{H^{++}}^2 - 6m_{H^+}^2 c_{2\beta}) \\ &\quad + (4m_A^2 + m_h^2 + m_H^2 - 12m_{H^+}^2 + 6m_{H^{++}}^2) s_\beta^{-2} - 3(m_h^2 - m_H^2) c_{2\alpha} (2 + s_\beta^{-2}), \\ 2\lambda'_{\beta 2} &= 9(m_A^2 + 2m_{H^+}^2 c_{2\beta} - 2m_{H^{++}}^2 + (2m_{H^+}^2 - m_{H^{++}}^2 - m_A^2) s_\beta^{-2}). \end{aligned} \quad (\text{B23})$$

Finally, the mass of the triply-charged Higgs boson is

$$m_{H^{3+}}^2 = \frac{3}{2}m_{H^{++}}^2 + \frac{1}{4}m_A^2 (1 - 3\rho). \quad (\text{B24})$$

In terms of mass parameters, c_6 is

$$c_6 m_h^2 = \frac{32m_A^4 s_\beta t_\beta^2}{3(2 - c_{2\beta})^2 [(m_h^2 + m_H^2 + (m_H^2 - m_h^2) c_{2\alpha}) s_\beta + \sqrt{3}(m_H^2 - m_h^2) s_{2\alpha} c_\beta]}. \quad (\text{B25})$$

The cubic couplings are

$$\begin{aligned} \lambda'_{hhh} &= 3m_h^2 \left(c_\alpha^3 (3c_\beta^{-1} - 2c_\beta) - \sqrt{3}s_\alpha^3 (2 - c_{2\beta}) s_\beta^{-1} \right) \\ &\quad + m_A^2 \left(c_\alpha (4 - 5c_{2\alpha}) c_\beta + c_\alpha^3 c_\beta^{-1} + 3\sqrt{3}s_\alpha (c_{2\alpha} + s_\beta^{-2} s_\alpha^2) s_\beta \right), \\ 4\lambda'_{hhH} &= 2(2m_h^2 + m_H^2) (2 - c_{2\beta}) \left(c_\alpha c_\beta^{-1} + \sqrt{3}s_\alpha s_\beta^{-1} \right) s_{2\alpha} \\ &\quad + m_A^2 \left(\sqrt{3}c_\alpha \left((8 - 12c_{2\alpha}) s_\beta - 3s_\beta^{-1} \right) + c_\beta^{-1} \left(3\sqrt{3}c_{3\alpha} t_\beta^{-1} + (2 + c_{2\beta}) s_\alpha - (4 + 5c_{2\beta}) s_{3\alpha} \right) \right). \end{aligned} \quad (\text{B26})$$

- [1] W. Kilian and J. Reuter, “The Low-energy structure of little Higgs models,” *Phys. Rev.* **D70** (2004) 015004, [arXiv:hep-ph/0311095 \[hep-ph\]](#).
- [2] C. Englert, A. Freitas, M. M. Muhlleitner, T. Plehn, M. Rauch, M. Spira, and K. Walz, “Precision Measurements of Higgs Couplings: Implications for New Physics Scales,” *J. Phys.* **G41** (2014) 113001, [arXiv:1403.7191 \[hep-ph\]](#).
- [3] B. Henning, X. Lu, and H. Murayama, “How to use the Standard Model effective field theory,” *JHEP* **01** (2016) 023, [arXiv:1412.1837 \[hep-ph\]](#).
- [4] J. de Blas, M. Chala, M. Perez-Victoria, and J. Santiago, “Observable Effects of General New Scalar Particles,” *JHEP* **04** (2015) 078, [arXiv:1412.8480 \[hep-ph\]](#).

- [5] M. Gorbahn, J. M. No, and V. Sanz, “Benchmarks for Higgs Effective Theory: Extended Higgs Sectors,” *JHEP* **10** (2015) 036, [arXiv:1502.07352 \[hep-ph\]](#).
- [6] J. Brehmer, A. Freitas, D. Lopez-Val, and T. Plehn, “Pushing Higgs Effective Theory to its Limits,” *Phys. Rev. D* **93** no. 7, (2016) 075014, [arXiv:1510.03443 \[hep-ph\]](#).
- [7] C.-W. Chiang and R. Huo, “Standard Model Effective Field Theory: Integrating out a Generic Scalar,” *JHEP* **09** (2015) 152, [arXiv:1505.06334 \[hep-ph\]](#).
- [8] M. Carena, I. Low, N. R. Shah, and C. E. M. Wagner, “Impersonating the Standard Model Higgs Boson: Alignment without Decoupling,” *JHEP* **04** (2014) 015, [arXiv:1310.2248 \[hep-ph\]](#).
- [9] J. F. Gunion and H. E. Haber, “The CP conserving two Higgs doublet model: The Approach to the decoupling limit,” *Phys. Rev. D* **67** (2003) 075019, [arXiv:hep-ph/0207010 \[hep-ph\]](#).
- [10] Z. U. Khandker, D. Li, and W. Skiba, “Electroweak Corrections from Triplet Scalars,” *Phys. Rev. D* **86** (2012) 015006, [arXiv:1201.4383 \[hep-ph\]](#).
- [11] F. del Aguila, Z. Kunszt, and J. Santiago, “One-loop effective lagrangians after matching,” *Eur. Phys. J. C* **76** no. 5, (2016) 244, [arXiv:1602.00126 \[hep-ph\]](#).
- [12] G. Buchalla, O. Cata, A. Celis, and C. Krause, “Standard Model Extended by a Heavy Singlet: Linear vs. Nonlinear EFT,” [arXiv:1608.03564 \[hep-ph\]](#).
- [13] Y. Jiang and M. Trott, “On the non-minimal character of the SMEFT,” [arXiv:1612.02040 \[hep-ph\]](#).
- [14] F. Feruglio, “The Chiral approach to the electroweak interactions,” *Int. J. Mod. Phys. A* **8** (1993) 4937–4972, [arXiv:hep-ph/9301281 \[hep-ph\]](#).
- [15] C. P. Burgess, J. Matias, and M. Pospelov, “A Higgs or not a Higgs? What to do if you discover a new scalar particle,” *Int. J. Mod. Phys. A* **17** (2002) 1841–1918, [arXiv:hep-ph/9912459 \[hep-ph\]](#).
- [16] B. Grinstein and M. Trott, “A Higgs-Higgs bound state due to new physics at a TeV,” *Phys. Rev. D* **76** (2007) 073002, [arXiv:0704.1505 \[hep-ph\]](#).
- [17] R. Contino, A. Falkowski, F. Goertz, C. Grojean, and F. Riva, “On the Validity of the Effective Field Theory Approach to SM Precision Tests,” *JHEP* **07** (2016) 144, [arXiv:1604.06444 \[hep-ph\]](#).
- [18] F. Ferreira, S. Fichet, and V. Sanz, “On new physics searches with multidimensional differential shapes,” [arXiv:1702.05106 \[hep-ph\]](#).
- [19] G. Heinrich, S. P. Jones, M. Kerner, G. Luisoni, and E. Vryonidou, “NLO predictions for Higgs boson pair production with full top quark mass dependence matched to parton showers,” [arXiv:1703.09252 \[hep-ph\]](#).
- [20] M. J. Dolan, C. Englert, and M. Spannowsky, “Higgs self-coupling measurements at the LHC,” *JHEP* **10** (2012) 112, [arXiv:1206.5001 \[hep-ph\]](#).
- [21] C.-Y. Chen, S. Dawson, and I. M. Lewis, “Exploring resonant di-Higgs boson production in the Higgs singlet model,” *Phys. Rev. D* **91** no. 3, (2015) 035015, [arXiv:1410.5488 \[hep-ph\]](#).
- [22] R. Contino, M. Ghezzi, M. Moretti, G. Panico, F. Piccinini, and A. Wulzer, “Anomalous Couplings in Double Higgs Production,” *JHEP* **08** (2012) 154, [arXiv:1205.5444 \[hep-ph\]](#).
- [23] F. Goertz, A. Papaefstathiou, L. L. Yang, and J. Zurita, “Higgs boson pair production in the D=6 extension of the SM,” *JHEP* **04** (2015) 167, [arXiv:1410.3471 \[hep-ph\]](#).
- [24] A. Azatov, R. Contino, G. Panico, and M. Son, “Effective field theory analysis of double Higgs boson production via gluon fusion,” *Phys. Rev. D* **92** no. 3, (2015) 035001, [arXiv:1502.00539 \[hep-ph\]](#).
- [25] M. J. Dolan, C. Englert, and M. Spannowsky, “New Physics in LHC Higgs boson pair production,” *Phys. Rev. D* **87** no. 5, (2013) 055002, [arXiv:1210.8166 \[hep-ph\]](#).
- [26] M. Bowen, Y. Cui, and J. D. Wells, “Narrow trans-TeV Higgs bosons and $H \rightarrow j \text{--} \bar{j} \text{--} hh$ decays: Two LHC search paths for a hidden sector Higgs boson,” *JHEP* **03** (2007) 036, [arXiv:hep-ph/0701035 \[hep-ph\]](#).
- [27] G. M. Pruna and T. Robens, “Higgs singlet extension parameter space in the light of the LHC discovery,” *Phys. Rev. D* **88** no. 11, (2013) 115012, [arXiv:1303.1150 \[hep-ph\]](#).
- [28] J. M. No and M. Ramsey-Musolf, “Probing the Higgs Portal at the LHC Through Resonant di-Higgs Production,” *Phys. Rev. D* **89** no. 9, (2014) 095031, [arXiv:1310.6035 \[hep-ph\]](#).
- [29] D. de Florian, I. Fabre, and J. Mazzitelli, “Higgs boson pair production at NNLO in QCD including dimension 6 operators,” [arXiv:1704.05700 \[hep-ph\]](#).
- [30] J. R. Forshaw, A. Sabio Vera, and B. E. White, “Mass bounds in a model with a triplet Higgs,” *JHEP* **06** (2003) 059, [arXiv:hep-ph/0302256 \[hep-ph\]](#).
- [31] R. S. Chivukula, N. D. Christensen, and E. H. Simmons, “Low-energy effective theory, unitarity, and non-decoupling behavior in a model with heavy Higgs-triplet fields,” *Phys. Rev. D* **77** (2008) 035001, [arXiv:0712.0546 \[hep-ph\]](#).
- [32] M.-C. Chen, S. Dawson, and C. B. Jackson, “Higgs Triplets, Decoupling, and Precision Measurements,” *Phys. Rev. D* **78** (2008) 093001, [arXiv:0809.4185 \[hep-ph\]](#).
- [33] C. Englert, E. Re, and M. Spannowsky, “Pinning down Higgs triplets at the LHC,” *Phys. Rev. D* **88** (2013) 035024, [arXiv:1306.6228 \[hep-ph\]](#).
- [34] S. S. AbdusSalam and T. A. Chowdhury, “Scalar Representations in the Light of Electroweak Phase Transition and Cold Dark Matter Phenomenology,” *JCAP* **1405** (2014) 026, [arXiv:1310.8152 \[hep-ph\]](#).
- [35] R. Contino, M. Ghezzi, C. Grojean, M. Muhlleitner, and M. Spira, “Effective Lagrangian for a light Higgs-like scalar,” *JHEP* **07** (2013) 035, [arXiv:1303.3876 \[hep-ph\]](#).

- [36] B. Grzadkowski, M. Iskrzynski, M. Misiak, and J. Rosiek, “Dimension-Six Terms in the Standard Model Lagrangian,” *JHEP* **10** (2010) 085, [arXiv:1008.4884 \[hep-ph\]](#).
- [37] E. E. Jenkins, A. V. Manohar, and M. Trott, “Renormalization Group Evolution of the Standard Model Dimension Six Operators I: Formalism and λ Dependence,” *JHEP* **10** (2013) 087, [arXiv:1308.2627 \[hep-ph\]](#).
- [38] E. E. Jenkins, A. V. Manohar, and M. Trott, “Renormalization Group Evolution of the Standard Model Dimension Six Operators II: Yukawa Dependence,” *JHEP* **01** (2014) 035, [arXiv:1310.4838 \[hep-ph\]](#).
- [39] R. Alonso, E. E. Jenkins, A. V. Manohar, and M. Trott, “Renormalization Group Evolution of the Standard Model Dimension Six Operators III: Gauge Coupling Dependence and Phenomenology,” *JHEP* **04** (2014) 159, [arXiv:1312.2014 \[hep-ph\]](#).
- [40] G. F. Giudice, C. Grojean, A. Pomarol, and R. Rattazzi, “The Strongly-Interacting Light Higgs,” *JHEP* **06** (2007) 045, [arXiv:hep-ph/0703164 \[hep-ph\]](#).
- [41] G. Buchalla, O. Cata, and C. Krause, “Complete Electroweak Chiral Lagrangian with a Light Higgs at NLO,” *Nucl. Phys.* **B880** (2014) 552–573, [arXiv:1307.5017 \[hep-ph\]](#). [Erratum: Nucl. Phys. B913,475(2016)].
- [42] ATLAS Collaboration, T. A. collaboration, “Constraints on New Phenomena via Higgs Coupling Measurements with the ATLAS Detector,”.
- [43] J. R. Espinosa, T. Konstandin, and F. Riva, “Strong Electroweak Phase Transitions in the Standard Model with a Singlet,” *Nucl. Phys.* **B854** (2012) 592–630, [arXiv:1107.5441 \[hep-ph\]](#).
- [44] J. Hisano and K. Tsumura, “Higgs boson mixes with an SU(2) septet representation,” *Phys. Rev.* **D87** (2013) 053004, [arXiv:1301.6455 \[hep-ph\]](#).
- [45] H. Belusca-Maito, A. Falkowski, D. Fontes, J. C. Romao, and J. P. Silva, “Higgs EFT for 2HDM and beyond,” *Eur. Phys. J.* **C77** no. 3, (2017) 176, [arXiv:1611.01112 \[hep-ph\]](#).
- [46] N. G. Deshpande and E. Ma, “Pattern of Symmetry Breaking with Two Higgs Doublets,” *Phys. Rev.* **D18** (1978) 2574.
- [47] D. A. Ross and M. J. G. Veltman, “Neutral Currents in Neutrino Experiments,” *Nucl. Phys.* **B95** (1975) 135–147.
- [48] J. Erler, “Precision Electroweak Measurements at Run 2 and Beyond,” 2017. [arXiv:1704.08330 \[hep-ph\]](#). <http://inspirehep.net/record/1597122/files/arXiv:1704.08330.pdf>.
- [49] Particle Data Group Collaboration, C. Patrignani *et al.*, “Review of Particle Physics,” *Chin. Phys.* **C40** no. 10, (2016) 100001.
- [50] H. Georgi and M. Machacek, “Doubly Charged Higgs Bosons,” *Nucl. Phys.* **B262** (1985) 463–477.
- [51] M. S. Chanowitz and M. Golden, “Higgs Boson Triplets With $M(W) = M(Z) \cos \theta_w$,” *Phys. Lett.* **B165** (1985) 105–108.
- [52] H. E. Logan and V. Rantala, “All the generalized Georgi-Machacek models,” *Phys. Rev.* **D92** no. 7, (2015) 075011, [arXiv:1502.01275 \[hep-ph\]](#).
- [53] G. Chalons, D. Lopez-Val, T. Robens, and T. Stefaniak, “The Higgs singlet extension at LHC Run 2,” in *Proceedings, 38th International Conference on High Energy Physics (ICHEP 2016): Chicago, IL, USA, August 3-10, 2016*. 2016. [arXiv:1611.03007 \[hep-ph\]](#). <http://inspirehep.net/record/1496646/files/arXiv:1611.03007.pdf>.
- [54] ATLAS, CMS Collaboration, G. Aad *et al.*, “Measurements of the Higgs boson production and decay rates and constraints on its couplings from a combined ATLAS and CMS analysis of the LHC pp collision data at $\sqrt{s} = 7$ and 8 TeV,” *JHEP* **08** (2016) 045, [arXiv:1606.02266 \[hep-ex\]](#).
- [55] V. Cacchio, D. Chowdhury, O. Eberhardt, and C. W. Murphy, “Next-to-leading order unitarity fits in Two-Higgs-Doublet models with soft \mathbb{Z}_2 breaking,” *JHEP* **11** (2016) 026, [arXiv:1609.01290 \[hep-ph\]](#).
- [56] B. Grinstein and P. Uttayarat, “Carving Out Parameter Space in Type-II Two Higgs Doublets Model,” *JHEP* **06** (2013) 094, [arXiv:1304.0028 \[hep-ph\]](#). [Erratum: JHEP09,110(2013)].
- [57] LHC Higgs Cross Section Working Group Collaboration, J. R. Andersen *et al.*, “Handbook of LHC Higgs Cross Sections: 3. Higgs Properties,” [arXiv:1307.1347 \[hep-ph\]](#).
- [58] K. Kannike, “Vacuum Stability of a General Scalar Potential of a Few Fields,” *Eur. Phys. J.* **C76** no. 6, (2016) 324, [arXiv:1603.02680 \[hep-ph\]](#).
- [59] B. W. Lee, C. Quigg, and H. B. Thacker, “Weak Interactions at Very High-Energies: The Role of the Higgs Boson Mass,” *Phys. Rev.* **D16** (1977) 1519.
- [60] A. Dedes, W. Materkowska, M. Paraskevas, J. Rosiek, and K. Suxho, “Feynman Rules for the Standard Model Effective Field Theory in R_ξ -gauges,” [arXiv:1704.03888 \[hep-ph\]](#).
- [61] E. W. N. Glover and J. J. van der Bij, “Higgs boson pair production via gluon fusion,” *Nucl. Phys.* **B309** (1988) 282–294.
- [62] T. Plehn, M. Spira, and P. M. Zerwas, “Pair production of neutral Higgs particles in gluon-gluon collisions,” *Nucl. Phys.* **B479** (1996) 46–64, [arXiv:hep-ph/9603205 \[hep-ph\]](#). [Erratum: Nucl. Phys. B531,655(1998)].
- [63] Q.-H. Cao, G. Li, B. Yan, D.-M. Zhang, and H. Zhang, “Double Higgs production at the 14 TeV LHC and the 100 TeV pp-collider,” [arXiv:1611.09336 \[hep-ph\]](#).
- [64] S. Dawson and I. M. Lewis, “NLO corrections to double Higgs boson production in the Higgs singlet

- model,” *Phys. Rev.* **D92** no. 9, (2015) 094023, [arXiv:1508.05397 \[hep-ph\]](#).
- [65] G. Cacciapaglia, H. Cai, A. Carvalho, A. Deandrea, T. Flacke, B. Fuks, D. Majumder, and H.-S. Shao, “Probing vector-like quark models with Higgs-boson pair production,” [arXiv:1703.10614 \[hep-ph\]](#).
- [66] L. Di Luzio, R. Grober, and M. Spannowsky, “Maxi-sizing the trilinear Higgs self-coupling: how large could it be?,” [arXiv:1704.02311 \[hep-ph\]](#).
- [67] S. Di Vita, C. Grojean, G. Panico, M. Riembau, and T. Vantalón, “A global view on the Higgs self-coupling,” [arXiv:1704.01953 \[hep-ph\]](#).
- [68] D. de Florian, M. Grazzini, C. Hanga, S. Kallweit, J. M. Lindert, P. Maierhofer, J. Mazzitelli, and D. Rathlev, “Differential Higgs Boson Pair Production at Next-to-Next-to-Leading Order in QCD,” *JHEP* **09** (2016) 151, [arXiv:1606.09519 \[hep-ph\]](#).
- [69] S. Borowka, N. Greiner, G. Heinrich, S. P. Jones, M. Kerner, J. Schlenk, and T. Zirke, “Full top quark mass dependence in Higgs boson pair production at NLO,” *JHEP* **10** (2016) 107, [arXiv:1608.04798 \[hep-ph\]](#).
- [70] CMS Collaboration, V. Khachatryan *et al.*, “Search for resonant pair production of Higgs bosons decaying to two bottom quark/antiquark pairs in proton/proton collisions at 8 TeV,” *Phys. Lett.* **B749** (2015) 560–582, [arXiv:1503.04114 \[hep-ex\]](#).
- [71] ATLAS Collaboration, G. Aad *et al.*, “Searches for Higgs boson pair production in the $hh \rightarrow bb\tau\tau, \gamma\gamma WW^*, \gamma\gamma bb, bbbb$ channels with the ATLAS detector,” *Phys. Rev.* **D92** (2015) 092004, [arXiv:1509.04670 \[hep-ex\]](#).
- [72] CMS Collaboration, C. Collaboration, “Model independent search for Higgs boson pair production in the $b\bar{b}\tau^+\tau^-$ final state,”.
- [73] CMS Collaboration, V. Khachatryan *et al.*, “Search for two Higgs bosons in final states containing two photons and two bottom quarks in proton-proton collisions at 8 TeV,” *Phys. Rev.* **D94** no. 5, (2016) 052012, [arXiv:1603.06896 \[hep-ex\]](#).
- [74] J. F. Owens, A. Accardi, and W. Melnitchouk, “Global parton distributions with nuclear and finite- Q^2 corrections,” *Phys. Rev.* **D87** no. 9, (2013) 094012, [arXiv:1212.1702 \[hep-ph\]](#).
- [75] W. Buchmüller and D. Wyler, “Effective Lagrangian Analysis of New Interactions and Flavor Conservation,” *Nucl. Phys.* **B268** (1986) 621–653.
- [76] A. Falkowski, B. Fuks, K. Mawatari, K. Mimasu, F. Riva, and V. Sanz, “Rosetta: an operator basis translator for Standard Model effective field theory,” *Eur. Phys. J.* **C75** no. 12, (2015) 583, [arXiv:1508.05895 \[hep-ph\]](#).
- [77] I. Low, R. Rattazzi, and A. Vichi, “Theoretical Constraints on the Higgs Effective Couplings,” *JHEP* **04** (2010) 126, [arXiv:0907.5413 \[hep-ph\]](#).